Title
Pyrolysis of Yttria Stabilized Zirconia and its Characterization

Permalink
https://escholarship.org/uc/item/43k6m0xc

Author
FARSHIHAGHRO, EBRAHIM

Publication Date
2013

Peer reviewed|Thesis/dissertation

UNIVERSITY OF CALIFORNIA
RIVERSIDE

Pyrolysis of Yttria Stabilized Zirconia and its Characterization

A Thesis submitted in partial satisfaction
of the requirements for the degree of

Master of Science

in

Mechanical Engineering

by

Ebrahim Farshihaghro

December 2013

Thesis Committee:
      Dr. Lorenzo Mangolini, Chairperson
      Dr. Javier Garay
      Dr. Guillermo Aguilar

The Thesis of Ebrahim Farshihaghro is approved:

_____

_____

_____
                                                    Committee Chairperson

University of California, Riverside

Acknowledgements

I would like to express my deepest gratitude to my advisor, Dr. Lorenzo Mangolini, for his encouragement and optimism throughout my graduate studies. I have learned a lot from him at our meetings and scientific discussions. This thesis would not have been possible without his support. I would also like to thank all of the members of the Dr. Mangolini's research group for their help and friendship.

I sincerely thank Dr. Javier Garay for his guidance and letting me do some parts of my research in his lab and for providing many valuable comments that improved the presentation and contents of this thesis.

Finally, and most importantly, I would like to thank my wife, Saharnaz, for her continued support, encouragement, patience and unwavering love. Her love is and always will be the biggest support for my entire life.

ABSTRACT OF THE THESIS

Pyrolysis of Yttria Stabilized Zirconia and its Characterization

by

Ebrahim Farshihaghro

Master of Science, Graduate Program in Mechanical Engineering
University of California, Riverside, December 2013
Dr. Lorenzo Mangolini, Chairperson

Most recently, there has been an increasing interest in transparent ceramics for applications in fields like optoelectronics, optomechanics, and optically activated drug delivery. Polycrystalline yttria stabilized zirconia (YSZ) is one of the most beneficial engineering ceramics. Zirconia in natural state is found in the form of baddeleyite. Phase transformations of pure undoped zirconia are mono-clinic phase, at room temperature, tetragonal phase, at 2400 °C and cubic phase at its melting point (2800 °C). However, it is difficult to produce ceramic parts with undoped zirconia because the sintering temperature of zirconia is at 1500 °C at which Zirconia is in mono-clinic phase.

The most common stabilizer to produce fired ceramic pieces is Y_2O_3. High hardness, toughness, and high oxygen diffusivity are among the versatile characteristics of YSZ.

Introducing optical transparency to this ceramic expands the range of applications for this material. Among important optical diagnostic and therapeutic applications one important application is the non-invasive light delivery and collection from shallow and deep brain tissues. Replacing YSZ implant over a portion of skull allows the real-time imaging, highly precise visualization, and treatment of brain tumor without the need of highly invasive craniotomies.

A new approach to produce yttrium stabilized zirconia has been introduced, in order to get optically transparent densified YSZ nanoparticles with average particle size of 10nm. Different nebulizers have been utilized in the Spray Pyrolysis set up and the effect of furnace temperature on the structure of produced zirconia and YSZ has been analyzed by X-ray Diffraction and Transmission Electron Microscopy method. The produced nanoparticles were densified utilizing CAPAD method. Annealing of the final densified YSZ improves the optical transparency of the samples.

Table of Contents

List of Figures

xi

List of Tables

Chapter 1

Introduction

1.1 General Overview

In this thesis a new approach to produce Yttrium stabilized Zirconia is introduced and the experimental results of characterizing these nanoparticles are presented. The experiments were conducted in Professor Lorenzo Mangolini's lab situated in the Mechanical Engineering Department of the University of California, Riverside, USA.

The following is a brief introduction of Zirconia nanoparticles, the procedures for stabilizing these nanoparticles continued with introducing Ytrrium Stabilized Zirconia, its applications, and phase diagram. The organization of this thesis is reviewed at the end of this chapter.

1.2 Zirconium dioxide

Most recently there has been an increasing interest in transparent ceramics for applications in fields like optoelectronics, optomechanics, and optically activated drug delivery. Transparent Al_2O_3 (alumina), $MgAl_2O_4$ (spinel), indium tin oxide (ITO), and

$Y_3Al_5O_{12}$ (YAG) are the most commonly studied materials. Polycrystalline yttria stabilized zirconia (YSZ) on the other hand is one of the most beneficial engineering ceramics. The main element of this configuration, Zirconia, is a ceramic material with prominent mechanical properties, which ensure a broad range of applications for it.

Zirconium dioxide (ZrO2), also known as zirconia, is a white crystalline oxide of zirconium as shown in Figure 1.1. In its natural form, it is the mineral baddeleyite and has a monoclinic crystalline structure. A dopant stabilized cubic structured zirconia, cubic zirconia, is synthesized in various colors for use as a gemstone and a diamond simulant.

Phase transformations of pure undoped zirconia are mono-clinic phase, from room temperature to 1175 °C, tetragonal phase, between 1175 and 2370 °C and cubic phase from 2370 °C to its melting point (2750 °C). The higher the temperature is the higher the symmetry gets.

Figure 1.1: White Zirconia powder
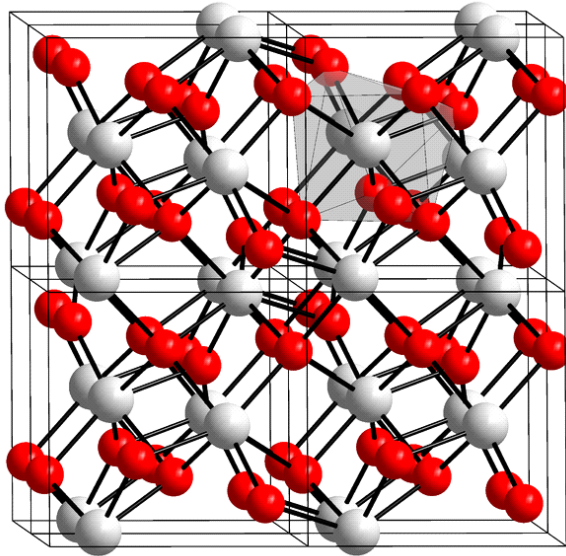
Figure 1.2: Crystal Structure of Zirconium (IV)-Oxide

However, it is difficult to produce ceramic parts with undoped zirconia because the sintering temperature of zirconia is at 1400 to 1500 °C. During the cooling, an inherent tetragonal-monoclinic transformation volume change occurs that causes some cracks on the final pieces.

Monoclinic zirconia consists of seven-coordinate zirconium centers, which are the result of the large size of Zr atoms as seen in Figure 1.2. When the zirconia is blended with some other oxides, the tetragonal and/or cubic phases are stabilized [1]. Effective dopants include magnesium oxide (MgO), yttrium oxide (Y_2O_3, yttria), calcium oxide (CaO), and cerium (III) oxide (Ce_2O_3) [2].

Generally the most useful state of Zirconia is the stabilized state. In order to remove the disruptive phase change during the heating procedure a few percentages of yttria can be

added to Zirconia. The resulting material will have dominant thermal, mechanical, and electrical properties. In some cases, the tetragonal phase can be metastable. If sufficient quantities of the metastable tetragonal phase is present, then an applied stress, magnified by the stress concentration at a crack tip, can cause the tetragonal phase to convert to monoclinic, with the associated volume expansion. This phase transformation can then put the crack into compression, retarding its growth, and enhancing the fracture toughness. This mechanism is known as transformation toughening, and significantly extends the reliability and lifetime of products made with stabilized zirconia [2][3]. The phase dependent band gap of ZrO_2 typically is from 5-7 eV [4]. A special case of zirconia is that of tetragonal zirconia polycrystal, or TZP, which is indicative of polycrystalline zirconia composed of only the metastable tetragonal phase.

Zirconia is most often used in the production of ceramics. Other applications of Zirconia include protective coating on particles of titanium dioxide pigments, refractory material, insulation, abrasives and enamels. Furthermore, oxygen sensors and fuel cell membranes use stabilized zirconia because of the ability of Zirconia in allowing oxygen ions to move freely through the crystal structure at high temperatures. As a result, it is one of the most useful electroceramics. Jet and diesel engines take advantage of very low thermal conductivity of cubic phase of zirconia as this material is used as a thermal barrier coating in their engines.

In dentistry on the other hand, Zirconia is being used in the manufacture of subframes for the construction of dental restorations such as crowns and bridges, and strong, extremely durable dental prostheses constructed entirely from monolithic zirconia.

For Zirconia's superior hardness, it is used to make ceramic knives. Zirconia based cutlery stays sharp longer than a stainless steel equivalent. Zirconia is also a potential high-k dielectric material with potential applications as an insulator in transistors.

As another application of Zirconia we can refer to its use in the deposition of optical coatings because it is a high-index material that can be used from the near-UV to the mid-IR. It has low absorption in this spectral region. It is typically deposited by physical vapor deposition (PVD) in these applications.

1.3 Yttria-stabilized zirconia

Yttria-stabilized zirconia (YSZ) is a zirconium-oxide based ceramic, in which the crystal structure of zirconium oxide is stabilized down to room temperature by an addition of yttrium oxide, avoiding the phase transitions that pure zirconia undergo during heating or cooling. These oxides are commonly called "zirconia" (ZrO_2) and "yttria" (Y_2O_3). Generally transitions that pure zirconia undergoes during heating or cooling is:

$$monoclinic \xrightarrow{1170^{\circ}C} tetragonal \xrightarrow{2350^{\circ}C} cubic \xrightarrow{2700^{\circ}C} liquid \qquad (1.1)$$
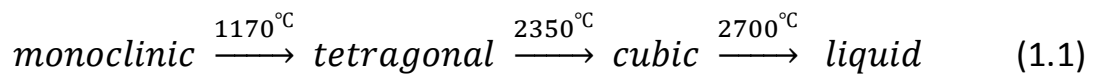
with the attendant volume changes and possible mechanical stresses or failures. Stabilization of the cubic polymorph of zirconia over wider range of temperatures is accomplished by substitution of some of the Zr^{4+} ions (ionic radius of 0.82 Å, too small for ideal lattice of fluorite characteristic for the tetragonal zirconia) in the crystal lattice with slightly larger ions, e.g., those of Y^{3+} (ionic radius of 0.96 Å).

Materials related to YSZ include calcia-, magnesia-, ceria- or alumina-stabilized zirconias, or partially stabilized zirconias (PSZ). Stabilized hafnia is also known.

Some of the abbreviations used in conjunction with stabilized zirconia are partly stabilized zriconia, and fully stabilized zirconia, ZrO_2. partly stabilized zriconias include PSZ, *partly stabilized zirconia,* TZP, *tetragonal zirconia polycrystal,* and 4YSZ with 4 mol-% Y_2O_3 partly stabilized ZrO_2. The last one is called *yttria stabilized zirconia* that can be seen in Figure 1.3.
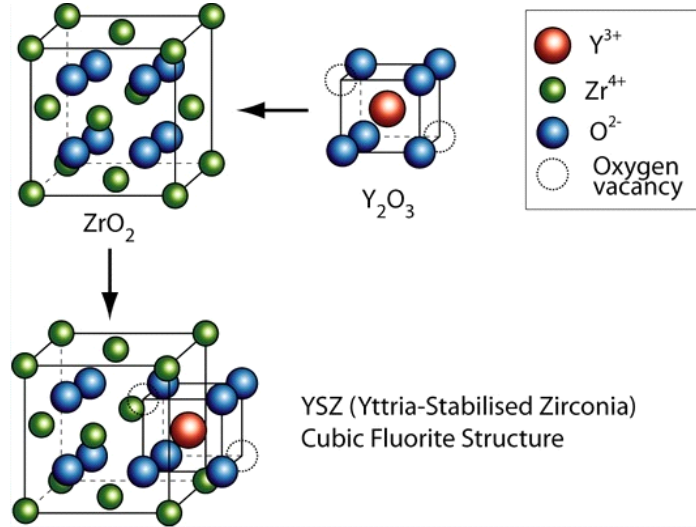
Figure 1.3: Structure of YSZ

Fully stabilized zirconias include, FSZ, fully stabilized zirconia, CSZ, cubic stabilized zirconia, 8YSZ - with 8 mol-% Y_2O_3 fully stabilized ZrO_2.

Doping zirconia with yttria has another effect which is to maintain neutrality by generating oxygen vacancies in the material. Addition of yttria to pure zirconia replaces some of the Zr^{4+} ions in the zirconia lattice with Y^{3+} ions. This produces oxygen vacancies, as three O^{2-} ions replace four O^{2-} ions. It also permits yttrium stabilized zirconia to conduct O^{2-} ions (and thus conduct an electrical current), provided there is sufficient vacancy site mobility, a property that increases with temperature. This ability to conduct O^{2-} ions makes yttria-stabilized zirconia well suited to use in solid oxide fuel cells, although it requires that they operate at high enough temperatures. The ionic conductivity of the stabilized zirconias increases with increasing dopant concentration (linearly for low dopant concentrations), then saturates, and then starts to decrease. The maximum ionic conductivity is obtained at Y_2O_3 concentration of about 8%(1000 °C) [5].

1.4 Applications of yttria-stabilized zirconia

One of the most common applications of YSZ is in tooth crowns for its hardness and chemical inertness. Furthermore, YSZ is being used as a refractory like in jet engines, as a thermal barrier coating in gas turbines, and as an electroceramic due to its ion-conducting properties. In its electroceramic form it can be used to determine oxygen content in exhaust gases or to measure pH in high-temperature water.

The other application of YSZ is in solid oxide fuel cell (SOFC). YSZ is used as the solid electrolyte, which enables oxygen ion conduction while blocking electronic conduction. In order to achieve sufficient ion conduction, an SOFC with a YSZ electrolyte must be operated at high temperatures (800 °C-1000 °C). While it is advantageous that YSZ retains mechanical robustness at those temperatures, overall the high temperature necessary is a disadvantage of current SOFCs, and is one of the major barriers to successful commercialization. The high density of YSZ is also necessary in order to physically separate the gaseous fuel from oxygen, or else the electrochemical system would produce no electrical power.

In water-based pastes Yttria-stabilized zirconia can be used in *do-it-yourself* ceramics and cements. These contain microscopic YSZ milled fibers or sub-micrometer particles, often with potassium silicate and zirconium acetate binders (at mildly acidic pH). The cementation occurs on removal of water. The resulting ceramic material is suitable for very high temperature applications.

YSZ doped with rare-earth materials can act as a thermographic phosphor and a luminescent material. Some other applications include its usage in Nernst lamps for glowing rods, in non-metallic knife blades, produced by Boker and Kyocera companies, and in high precision alignment sleeve for optical fiber connector ferrules.

Introducing optical transparency to this ceramic expands the range of applications of this material even more. Among important optical diagnostic and therapeutic applications, its usage in non-invasive light delivery and collection from shallow and deep brain tissues can be mentioned. Replacing YSZ implant over a portion of skull allows the real-time imaging, highly precise visualization, and treatment of brain tumor without the need of highly invasive craniotomies.

1.5 Phase Diagram of YSZ

As mentioned before, zirconia (ZrO_2) at ambient pressures occurs in three polymorphic forms: monoclinic at room temperature, tetragonal at higher temperatures, and cubic at yet higher temperatures. Yttria (Y_2O_3) is added to zirconia to stabilize the intermediate temperature tetragonal phase (so-called partially stabilized zirconia, approximately 8% by mass Y_2O_3 equivalent to 8.7 mol% $YO_{1.5}$) or the high-temperature cubic phase (fully stabilized zirconia, with higher contents of Y_2O_3) at room temperature. Since the ZrO_2-Y_2O_3 ceramics have been used extensively in various applications, this material has attracted the interest of many researchers.

According to the phase diagram of ZrO_2-Y_2O_3 (Fig 1.4) the room temperature phase of ZrO_2 containing 8% by mass Y_2O_3 (8.7 mol% $YO_{1.5}$) is tetragonal. There is a two-phase region at temperatures between approximately 600 °C and 2000 °C where the phase composition is a mixture of cubic and tetragonal phases. At higher temperatures the stable phase is cubic [6].

The calculation of yttria content within the cubic and tetragonal phases was based on the changes of lattice parameters as described by Scott [6]. These data have been reinterpreted by Howard [7] to give the following relationships for the cubic phase, where a is the cubic lattice parameter:

$$\text{mol\% } YO_{1.5} = (a - 5.1159) / 0.00154 \qquad\qquad 1.2$$

and,

$$mol\% \quad YO_{1.5} = (1.0225 - c/a) / 0.001311 \qquad\qquad 1.3$$

for the tetragonal phase, where the ratio c/a of the tetragonal lattice parameters is calculated for an **F**-centered lattice. However, the total yttria content calculated using these expressions has been found to be greater than the nominal composition in several studied materials, most probably due to unrecognized cubic phase content in the presumed phase-pure tetragonal materials [8].
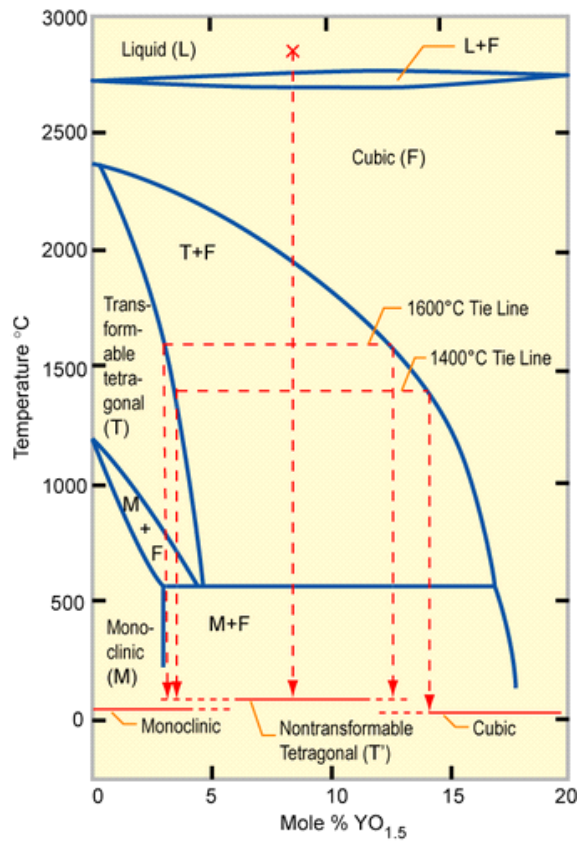
Figure 1.4: Phase diagram of YSZ

11

Since the cubic phase typically has a higher yttria content than the tetragonal phase, the scaling factor for the tetragonal phase was empirically adjusted to obtain results with the overall level of yttria content equal to the nominal composition of a wide range of samples, so that

$$\text{mol\% } YO_{1.5} = (1.0225 - c/a) / 0.0016 \qquad\qquad 1.4$$
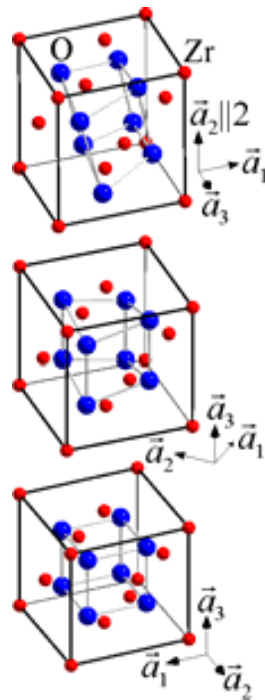
Fig 1.5: (a) monoclinic Yttria Stabilized Zirconia crystallises. (b) Tetragonal Partially Yttria Stabilized Zirconia. (c) Cubic Full Yttria Stabilized Zirconia [6]

1.6 YSZ Manufacturing

Ultra fine particles of YSZ can be manufactured via variety of methods including, but not limited to solution based methods like sol-gel, emulsion and colloidal, spray pyrolysis, salt assisted aerosol decomposition, carbon nanotube template method, mechanochemical processing, and thermal or non-thermal plasma techniques.

The sol-gel approach among others is a cheap and low-temperature technique. Products' chemical composition can be controlled precisely, which enables the application of this technique in manufacturing and processing the ceramics that can be used as an investment casting material. The other beneficial application of this approach is its usage as a means of producing very thin films of metal oxides for various purposes. Furthermore, Sol-gel derived materials can be employed in optical instruments, space devices, energy products, electronics, variety of sensor types, medicine and future generation of single molecule detectors.

On the other hand, plasma spraying, a branch of thermal spray processes is a layer by layer deposition technique that enables a large selection of materials. Very high cooling rate and high deposition rate are some other characteristics of this technique that make it more attractive for commercial applications.

Spray pyrolysis is a process well suited to the production of YSZ submicron powders. The control of the primary particle diameter using the process parameters is one of the most important advantages of this synthesis method. Submicron spherical particles can be easily obtained with this method. In addition, while all spherical aerosol droplets are

separately pyrolysed in a short time to form discrete solid particles, a good dispersion of these powders in any solvent is very easy to achieve in comparison to powders from other methods such as sol–gel or co-precipitation.

We will introduce a kind of spray pyrolysis method which will be explained in detail in chapter 2 on our method of YSZ production.

1.7 Organization of the thesis

Chapter 2 will describe the possible manufacturing procedures for YSZ in detail and the one that has been used for the present work. In chapter 3 the experimental results are presented and discussed. Conclusions and recommendations for future work are given in chapter 4.

References

[1] Nielsen, R., Zirconium and Zirconium Compounds, Ullmann's Encyclopedia of Industrial Chemistry, (2005).

[2] Evans, A.G., Cannon, R.M. Acta Met. 34: 761 (1986).

[3] Porter, D.L., Evans, A.G., Heuer, A.H., Transformation toughening in PSZ, (1979).

[4] Jane, C., Lin, Y.S., Chu, K., Journal of Vacuum Science & Technology, (2001).

[5] American Ceramic Society, John Wiley and Sons. pp. 139, (2011).

[6] Scott, H.G., J. Mater. Sci. 10 1527-1535, (1975).

[7] Howard, C.J., Australian Nuclear Science and Technology Organization, (1998).

[8] Argyriou, D.N. , Howard, C.J., J. Appl. Cryst. 28 206-208, (1995).

Chapter 2

YSZ Manufacturing

2.1 Introduction

In this chapter, the most widely used methods for synthesizing zirconia nanoparticles are intruduced and the application of each method in manufactoring yttrium stabilized zirconia is analyzed.

Generally, there are several methods for creating nanoparticles, including:

- Solution based methods like sol-gel, colloidal and emulsion

- Spray pyrolysis

- Salt assisted aerosol decomposition

- Carbon nanotube templated method

- Mechanochemical processing

- Thermal and non-thermal plasma technique

2.2 Sol-Gel Method

The sol-gel process is a wet-chemical technique. This technique has a wide range of applications in the fields of materials science and ceramic manufacturing. The method is mainly used for the fabrication of metal oxides. It starts with conversion of monomers into a colloidal solution called sol. The solution acts as the precursor for an integrated network of either discrete particles or network polymers. The integrated network is called gel. Typical precursors are metal alkoxides and metal chlorides. Formation of a metal oxide involves connecting the metal centers with oxo (M-O-M) or hydroxo (M-OH-M) bridges, therefore generating metal-oxo or metal-hydroxo polymers in solution. The sol evolves towards the formation of a gel-like diphasic system containing both a liquid phase and solid phase whose morphologies range from discrete particles to continuous polymer networks.

In the case of the colloid, the volume fraction of particles (or particle density) may be so low that a significant amount of fluid may need to be removed initially for the gel-like properties to be recognized. This can be accomplished in any number of ways. The most simple method is to allow time for sedimentation to occur, and then pour off the remaining liquid. Centrifugation can also be used to accelerate the process of phase separation.

Removal of the remaining liquid (solvent) phase requires a drying process, which is typically accompanied by a significant amount of shrinkage and densification. The rate at which the solvent can be removed is ultimately determined by the distribution of porosity

in the gel. The ultimate microstructure of the final component will clearly be strongly influenced by changes implemented during this phase of processing. One of the distinct advantages of using this methodology as opposed to the more traditional processing techniques is that densification is often achieved at a much lower temperature.

The sol-gel approach is a cheap and low-temperature technique that allows for the fine control of the product's chemical composition. It can be used in ceramics processing and manufacturing as an investment casting material, or as a means of producing very thin films of metal oxides for various purposes. Sol-gel derived materials have diverse applications in optics, electronics, energy, space, (bio)sensors, medicine (e.g. controlled drug release) and separation (e.g. chromatography) technology.

The Sol-gel method can be used in producing ZrO_2 nanoparticles. The process usually starts with zirconium isopropoxide ($Zr(i\text{-}OC_3H_7)_4$). Zirconium propoxide ($Zr(n\text{-}OC_2H_7)_4$) and zirconium butoxide ($Zr(n\text{-}OC_4H_9)_4$) also are constantly used as precursors. Powders that are produced in this manner are uniform and well dispersed [2]. One of the problems with this process is that it is complicated and difficult to control, because the zirconium alkoxides are generally derived from $ZrCl_4{}^9$ and must be kept away from water. To overcome this problem Yuqun Xie at Hangzhou University has used a new Sol-gel method to prepare ultrafine ZrO_2 particles with the average size of ≈12 nm (Fig 2.1) [1].

In his study, zirconyl chloride ($ZrOCl_2{}^9$), which is an inorganic salt, was used as a precursor. The principle is that there is a hydrolysis equilibrium in the aqueous $ZrOCl_2$ solution [1]:

$$ZrOCl_2 + 2H_2O \Leftrightarrow ZrO(OH)_2 + 2HCl \quad \text{(hydrolysis)} \qquad\qquad 2\text{-}1$$

For this example a sol or gel of $ZrO(OH)_2$ can be formed directly from an inorganic compound.
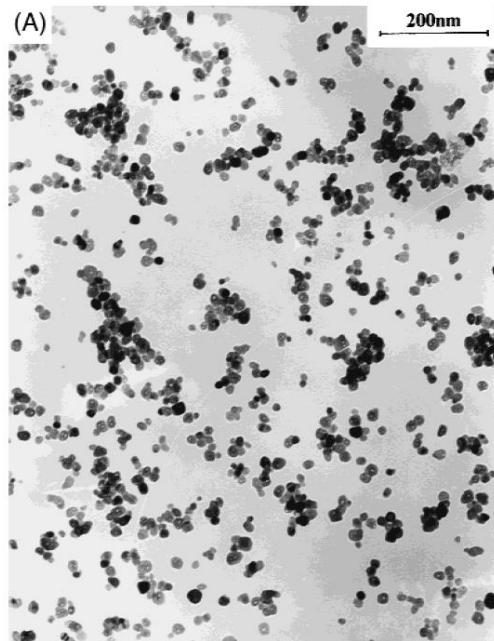
Fig 2.1: TEM micrographs of ZrO_2 calcined at 600°C for 3 h [1]

The process involves addition of excess C_2H_4O into the aqueous $ZrOCl_2$ solution and reacting the mixture at room temperature; a glassy $ZrO(OH)_2$ gel is formed moments later. An ultrafine ZrO_2 powder is obtained after the gel is dried and calcined at 600°C; the powder is monoclinic. The specific surface area of particle is 55.1 m^2/g. In addition, yttria-stabilized zirconia can be similarly prepared using the same process by adding 8 mol% of YCl_3 into a $ZrOCl_2$ solution.

2.3 Colloidal Method

Generally, the term colloid describes an extended range of solid–liquid (and/or liquid–liquid) mixtures. All of these mixtures contain distinct solid (and/or liquid) particles, which are dispersed in a liquid medium. Colloid term is referred to the particles that are larger than atomic dimensions but small enough to exhibit Brownian motion. If the particles are large enough, forces of gravity and sedimentation will govern their dynamic behavior in any given period of time in suspension. But if they are small enough to be colloids, their irregular motion in suspension can be attributed to the collective bombardment of a myriad of thermally agitated molecules in the liquid suspending medium, as described originally by Albert Einstein in his dissertation. Einstein proved the existence of water molecules by concluding that this erratic particle behavior could adequately be described using the theory of Brownian motion, with sedimentation being a possible long-term result. This critical size range (or particle diameter) typically ranges from nanometers (10^{-9} m) to micrometers (10^{-6} m) [3].

Oleg Vasylkiv and Yoshio Sakka's experiment is an example of synthesis and colloidal processing of zirconia nanopowder [4]. They have produced nanosized tetragonal 3 mol% Y_2O_3-doped ZrO_2 powder by hydrothermal precipitation from metal chlorides and urea solution. A washing–drying treatment and calcination, follows their procedure. They also showed the effects of powder washing by water and ethanol with subsequent centrifuging, and possible deagglomeration using microtip ultrasonication over powder properties in their experiment. Ultrasonic irradiation induced pressure waves generate

violently collapsible cavities that produces intense stress. This stress was used to minimize secondary particle size, deagglomerate the powder, re-disperse the ZrO_2 after all the washing–centrifuging cycles, and minimize mean aggregate size after final calcination. A uniformly aggregated tetragonal ZrO_2 nanopowder with a mean secondary particle size of ~ 45 nm, without hard agglomerates was prepared. Determination of the best suspension parameters allowed for low-temperature sinterability, which resulted in a nanograined ~ 95 nm ceramic (Fig 2.2) [4].
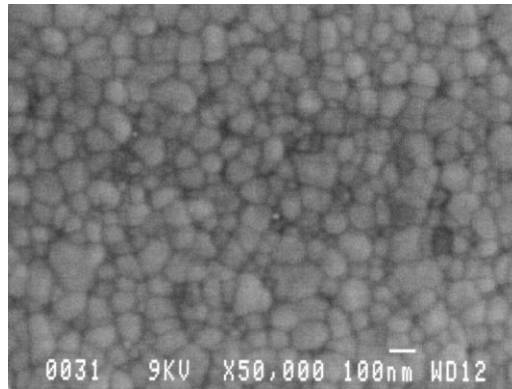

Fig 2.2: SEM micrograph of 3Y-TZP ceramic sintered at 1150°C for 60 h from uniformly aggregated urea-derived powder.

2.4 Emulsion Method

Microemulsion method was first introduced as an effective process of preparing nano-particles in the 1980's [5]. Reactants are solved in micro-droplets, which in turn act as

nano-reactors in the microemulsion system. When the reactors collide with each other, the precipitation reaction occurs. Then spherical powder with uniform size distribution and good dispersibility can be obtained. The particle size can be controlled via adjusting the size of reactors or other reaction conditions.

Lee et al. [6] produced microparticles of ZrO_2 using precipitation method between two emulsion solutions. In their experiment, two solutions of stable reverse emulsion (water-in-oil) are prepared and mixed to form gelled precipitates, using normal heptane as the continuous oil phase and aqueous solutions of zirconium oxyacetate and aqueous ammonia as the suspending droplets. Through a series of operations, including distillation, filtration and washing, the dried precursors are obtained. ZrO_2 powder with a tetragonal structure was obtained after calcining the precursors at $750^{\circ C}$.

In the two-emulsion technique (Fig 2.3), aqueous solution containing metal or aqueous ammonia is suspended in the oil phase to form emulsion by adding a surfactant or a mixture of surfactants. After preparing them separately, they are mixed together with agitation.

The advantage of the two-emulsion technique is the achievement of a uniform concentration of ammonia in the oil phase regardless of the contact mechanism as compared with the bubbling technique [6].
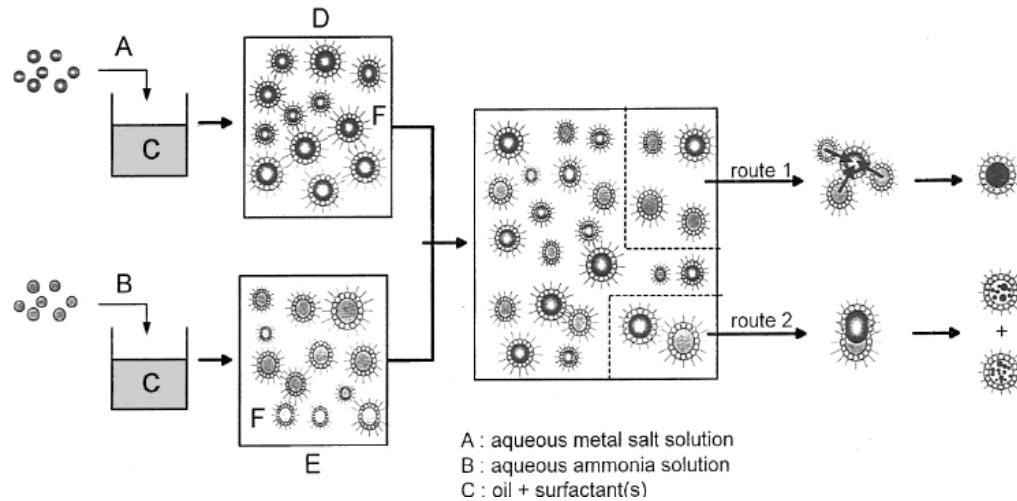
Fig 2.3: possible mechanisms of particle formation in two reverse emulsion precipitation method. A: aqueous metal salt solution, B: aqueous ammonia solution, C: oil + surfactant(s), D: reverse emulsions of aqueous metal salt solution, E: reverse emulsions of aqueous ammonia solution, F: oil.

During the reaction, nucleation, crystal growth and nulei agglomeration occur in the droplets which act as microreactors. Thus, the size, size distribution, and shape of produced particles from emulsion precipitation are related to the emulsion droplets and can be controlled better than the conventional precipitation, in which two solutions of reactant are mixed directly. Since the diffusion rate of ammonia is slow for route 1, the supersaturation generated by reaction in dr   e a chance to grow to large particles. On the other hand, the supersaturation is high in the droplets generated by the coaleascence of different types of droplets as route 2. In this case, there will be a larger number of smaller crystals, but they tend to form agglomerates. As a result, some of the precursor particles are larger than the emulsion

droplets.

Fig 2.4 shows the flowchart for preparing Zirconia powder by the two-emulsion technique [6].

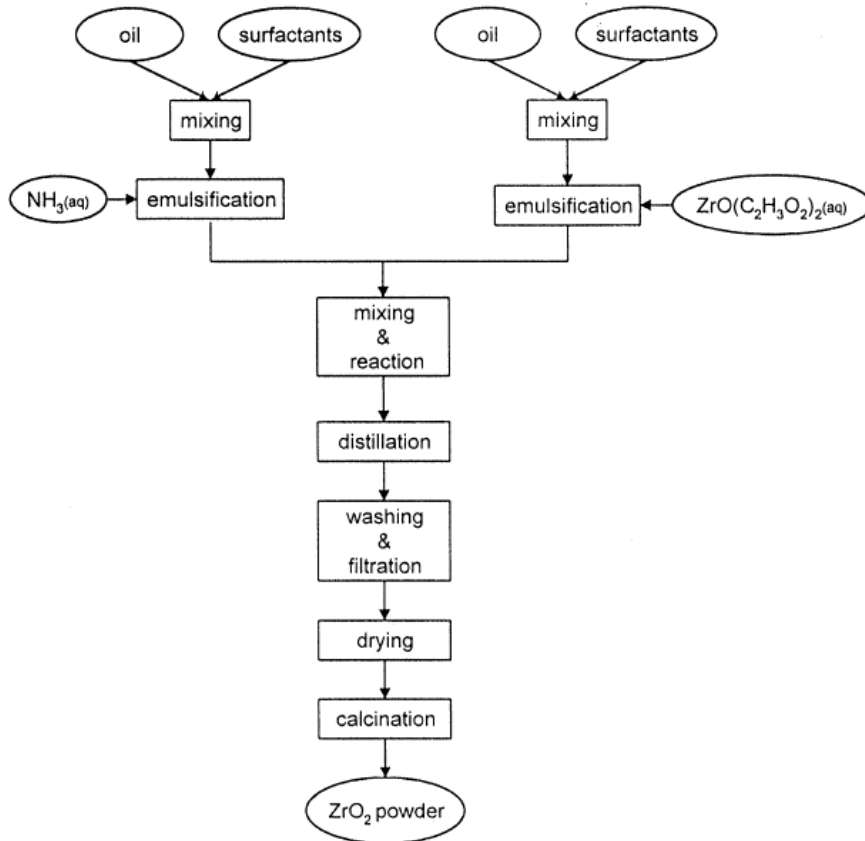Fig 2.4: Flowchart for preparing ZrO_2 powder by the two-emulsion technique.

There are many factors, including type and concentration of surfactant, type of oil phase, ratio of water to oil phase, and concentration of aqueous phase, that affect the characteristics of emulsion, which would subsequently influence the properties of the particles produced. From the practical point of view, the factors that influence the product

yield are significant, including the concentration of aqueous phase and the ratio of water/oil, which are usually not high for a stable emulsion. Four kinds of anionic surfactants are put to test for emulsion stability; among them Span 40 and Span 80 are considered as suitable surfactants for producing spherical microparticles of ZrO_2, which has a size range from several hundred nanometers to micrometers depending on the synthesis conditions.

Qiu et al. [8] on the other hand, took xylol/Tween 80/zirconium (yttrium) nitrate aqueous solution to prepare a microemulsion system. Spindle or approximate spherical powder was obtained through the reaction, which took place while ammonia gas was introduced into the system. The powder still had some pitfalls such as severe conglobation and large second particle size of 0.3–1.0 μm. Yang et al. [9] employed a water/cyclohexane microemulsion system and prepared a pure zirconia powder with the diameter lower than 10 nm and the specific area up to 197 m^2/g. The powder could be utilized as an adsorbent or a carrier of catalyst. Furthermore, cyclohexane/ TritonX-100/pentanol/water was taken by Tang et al. [10] as a microemulsion via which ultrafine spindle zirconia powder of monoclinic with the diameter 4–20 nm was prepared while a relative low reactant concentration was employed.

2.5 Spray Pyrolysis Method

In spray pyrolysis (SP) method, a vaporous precursor (liquid or gas) is forced through an orifice at high pressure and burned. The resulting solid is air classified to recover oxide

particles from by-product gases. Pyrolysis often results in aggregates and agglomerates rather than single primary particles. In principle, solution-based aerosol processes, unlike most solution processes, integrate the precipitation, thermolysis (i.e., calcination), and sintering stages of powder synthesis into a single continuous process. In this manner, the advantages of starting with a solution are complemented by providing unique control over the thermolysis and sintering stages of inorganic particle formation.

Spray pyrolysis (SP) has been widely used to describe these processes. However, the use of pyrolysis is sometimes too limiting and, in some cases, incorrectly describes the critical thermal process during SP. For example, pyrolysis (i.e., thermal decomposition) does not adequately capture the various oxidation, nitridation, or reduction-based thermal processes that will be increasingly important applications of SP type processes.

Spray drying, a process similar to SP, has been used for many years to produce pressing-grade ceramic powders and for numerous other applications in the foods, chemicals, and materials industries [9]. SP synthesis differs from spray drying in the use of solutions, the consequent process of precipitation or condensation within a droplet, and the use of significantly higher temperatures (e.g., $>3OO°C$) to form the desired inorganic phase by thermolysis.

During SP, the solution is atomized into a series of reactors (Fig. 2.5) where the aerosol droplets undergo evaporation and solute condensation within the droplet, drying, thermolysis of the precipitate particle at higher temperature to form a microporous particle, and, finally, sintering of the microporous particle to form a dense particle [10].

2.5.1 Atomization

A variety of atomization techniques such as pneumatic (pressure, two-fluid, nebulizers), ultrasonic, and electrostatic can be used for solution aerosol formation. These atomizers differ in droplet size, rate of atomization, and droplet velocity (Table 2.1).

The concept of SP processes is to produce one particle per droplet. Because small particles are required for most advanced ceramic applications, there is a serious need to develop techniques that can atomize large quantities of small droplets at low exit velocities. This is the reason why companies prefer pressure atomizers to ultrasonic atomizers. For a specific atomizer, the droplet characteristics depend on the solution density, viscosity, and surface tension.

Table 2.1 Characteristics of Atomizers CommonlyUsed for SP [10]

Atomizer	Droplet size (μm)	Atomization rate (cm^3/min)	Droplet velocity (m/s)
Pressure	10-100	3-no limit	5-20
Nebulizer	0.1-2	0.5-5	0.2-0.4
Ultrasonic	1-100	<2	0.2-0.4
Electrostatic	0.1-10		

2.5.2 Evaporation Period

During the first stage of SP, evaporation of the solvent from the surface of the droplet, diffusion of the solvent vapors away from the droplet in the gas phase, shrinkage of the droplet, change in the droplet temperature, and diffusion of solute toward the center of the droplet can occur simultaneously (Fig 2.5) [10].
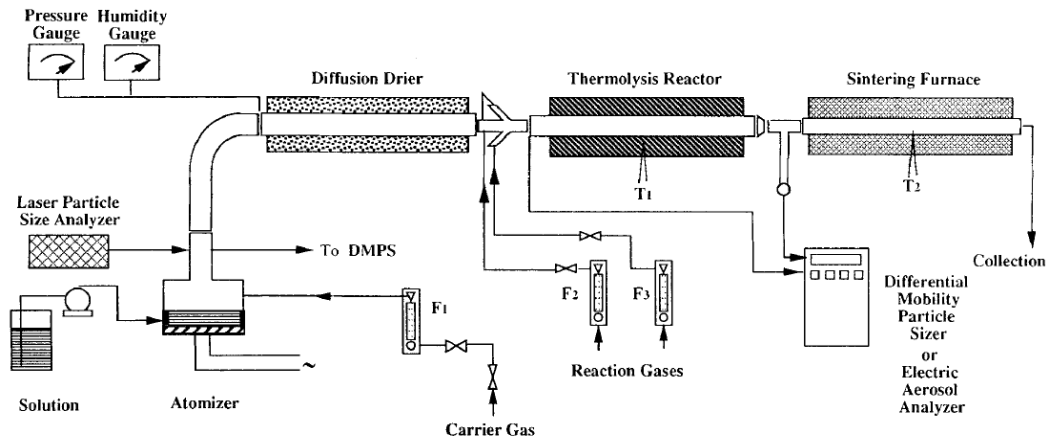

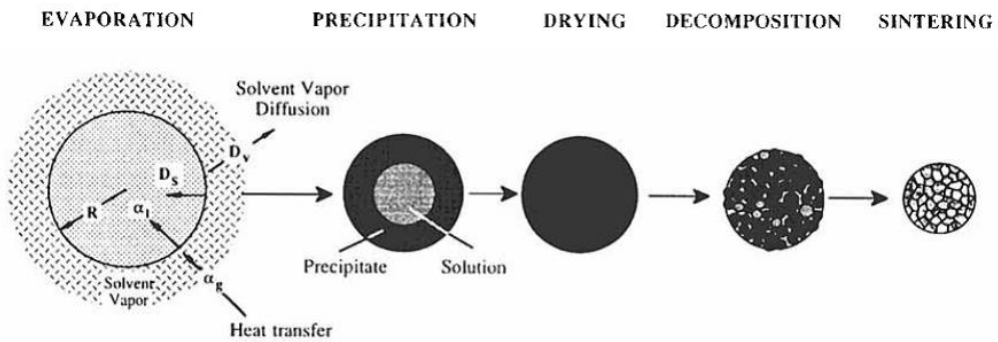Fig 2.5.1: Schematic of SP equipment [10]

Fig 2.5.2: Stages of SP Process

2.5.3 Thermolysis and Sintering

Since the SP particles are reactive after thermolysis, they should be sintered in situ to take full advantage of the SP process. Up to now, most reactor systems have been designed such that thermolysis and sintering processes overlap, i.e., a conventional, single-chamber spray drier is used. It is believed that the processes of evaporation, thermolysis, and sintering should be conducted in separate reactors to obtain maximum control of the individual processes and because the time-temperature conditions are significantly different. For example, thermolysis reactions take place at 400°C to 500°C, whereas sintering may take place at > 1000°C [10]. Overlap of these processes in a single droplet could significantly affect densification of the particle.

M Eslamian et al. [11] analyzed the effect of temperature on zirconia particle size and morphology. Their experiment shows that at high reactor temperatures ($\sim 400^{\circ}$C), the evaporation rate is much faster than the solute diffusion inside the droplet. As a result, a high solute concentration gradient develops within the droplet, which favors the formation of hollow particles. The final particle size increases with increasing reactor temperature. Low reactor temperatures ($<200^{\circ}$C) favor the formation of smaller particles (Fig 2.6). Reducing the droplet size from several microns to submicron size, or reducing the reactor pressure below 250 Torr, enhance the non-continuum effects, which reduces the evaporation rate. This results in the formation of fully filled particles. Basic steps of their spray pyrolysis method for zirconium hydroxychloride (ZrO(OH)Cl) production is shown in Fig 2.7.
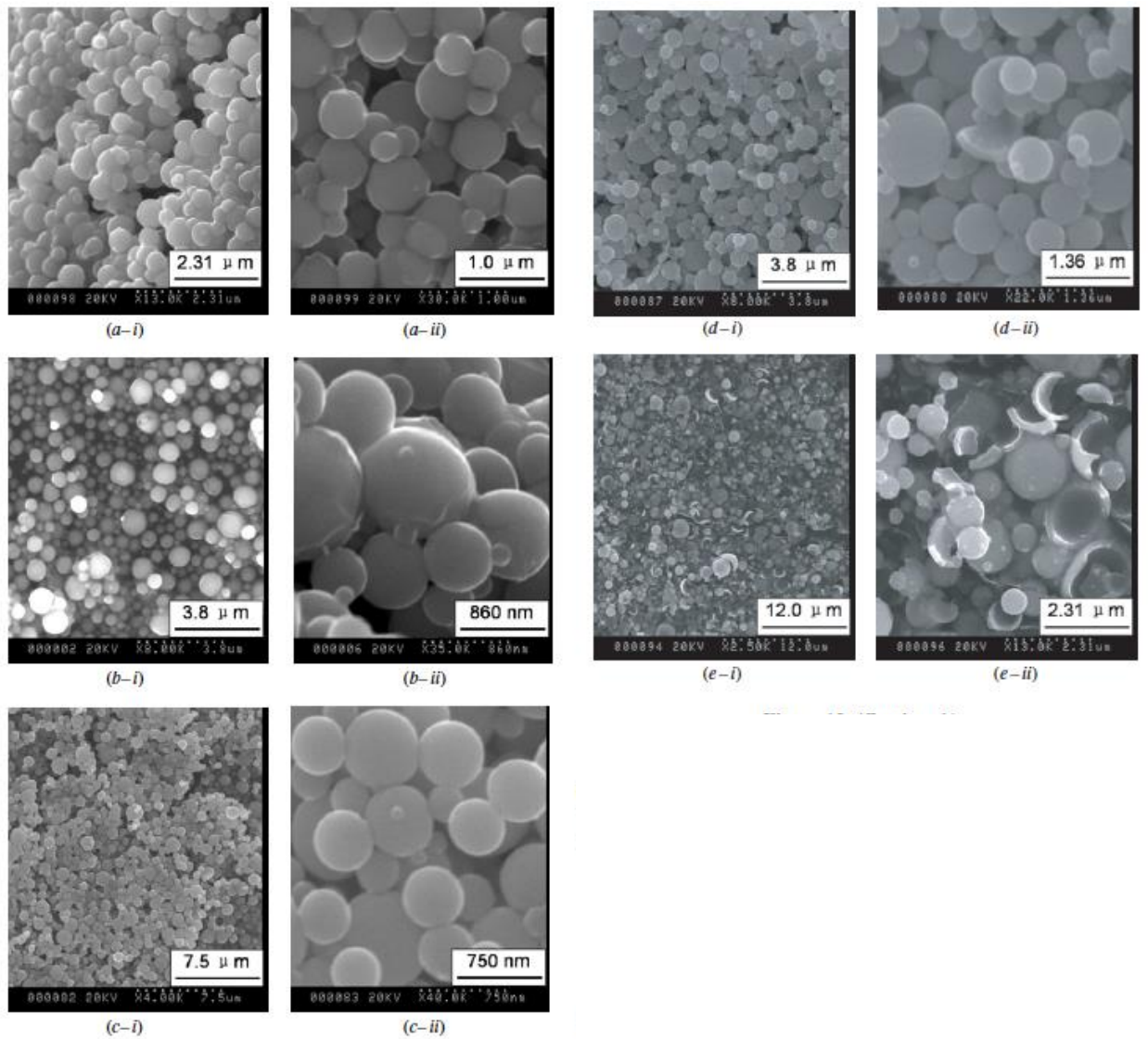
Fig 2.6: Scanning electron microscope (SEM) micrographs of zirconia particles prepared by spray pyrolysis using a 0.16 M solution of zirconium hydroxychloride (ZrO(OH)Cl) at (a) 70 ∘C, (b) 100 ∘C, (c) 200 ∘C, (d) 300 ∘C, and (e) 400 ∘C. The average particle sizes are 0.5, 0.58, 0.62, 0.70, and 0.74 μm, for (a)–(e) respectively.
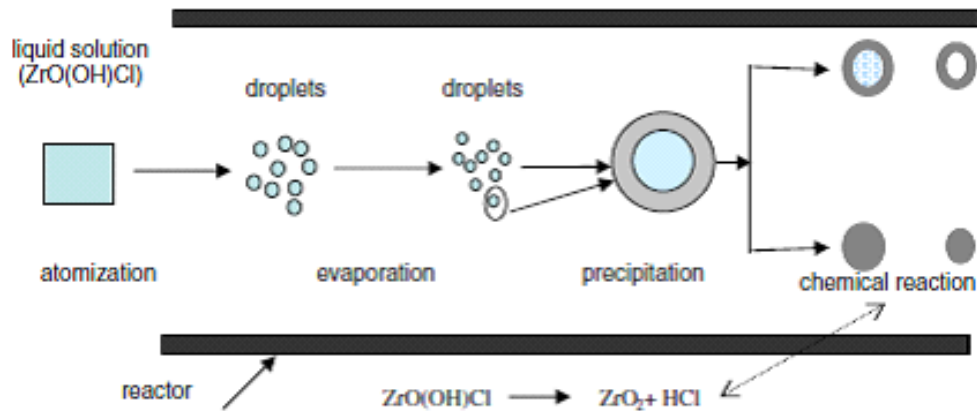
Fig 2.7: Basic steps of spray pyrolysis method for zirconium hydroxychloride (ZrO(OH)Cl). Once the (ZrO(OH)Cl) powders are relatively dried, they decompose to ZrO_2 and HCl. ZrO_2 powders remain in the collector and HCl gas goes to the ambient air.

2.6 Synthesis of YSZ powders by spray pyrolysis

Spray pyrolysis is a process well suited to the production of YSZ submicron powders, since it is a method that allows the synthesis of complex oxides at low temperatures which leads to submicron powders.

The control of the primary particle diameter using the process parameters is one of the most important advantages of this synthesis method for producing YSZ nanoparticles. Submicron spherical particles can be easily obtained. Furthermore, while all spherical aerosol droplets are separately pyrolysed in a short time to form discrete solid particles, a good dispersion of these powders in any solvent is very easy to obtain in comparison to powders from other methods such as sol–gel or co-precipitation.

Gaudon M. et al. [12] prepared 8-YSZ zirconia powders by the spray pyrolysis technique using an ultrasonic atomiser. They prepared precursor solutions from a stoichiometric mixture of zirconyl nitrate hydrate $ZrO(NO_3)_2 \cdot 6H_2O$ and yttrium nitrate hydrate $Y(NO_3)_3 \cdot 6H_2O$ dissolved in distilled water. The concentration was fixed to 2.5×10^{-2} mol l^{-1}. The procedure was followed by atomising the solutions by a high-frequency ultrasonic mist generator. In their study, two piezoelectric ceramic transducers with frequencies equal to 2.5 and 1.7 MHz were used. Their atomisers contained three ceramic transducers. The produced aerosol was carried through a tubular furnace with air (N_2–O_2 mixture) flow rate of 6l min^{-1}. The temperature of the tubular furnace was fixed at 600 or $1100^{\circ C}$.

From the studies in the literature about the influence of synthesis parameters on the transformation step from aerosol droplets to solid particles, it can be concluded that four parameters shoud be considered in that respect including, the atomizing frequency of the piezoelectric ceramics, the concentration of metallic salts in the starting solution, the flow rate of the aerosol in the tubular furnace, and the furnace temperature [13-14].

Gaudon M. et al. [12] showed that the higher the spray pyrolysis temperature, the denser the particles; i.e. the larger the densification. Furthermore, synthesis of dense particles leads to ceramics, which are easier to densify at relatively low temperatures.

Dubois B. et al. [15] prepared 3Y-TZP particles in the range 0.2 to1.8 pm were prepared by the spray pyrolysis of aqueous solutions of zirconyl chloride and yttrium nitrate using an ultrasonic mist generator. Figure 2.8 shows the schematic diagram of the apparatus they used for powder preparation. The starting materials, $ZrOCl_2.8H_2O$ and $Y(NO_3)_3.6H_2O$

(3 mol%), were dissolved in an aqueous solution. The mean size of droplets was 5 and 2 μm for 800 kHz and 2.5 kHz ultrasonic transducer frequencies, respectively. The mean size was determined by [15],

$$\overline{d} = \sqrt[3]{\frac{\rho s}{4 r f^2}}$$

2.2

where σ is the surface tension of the solution, r is the density of the solution, and f is the frequency of the ultrasonic transducer.
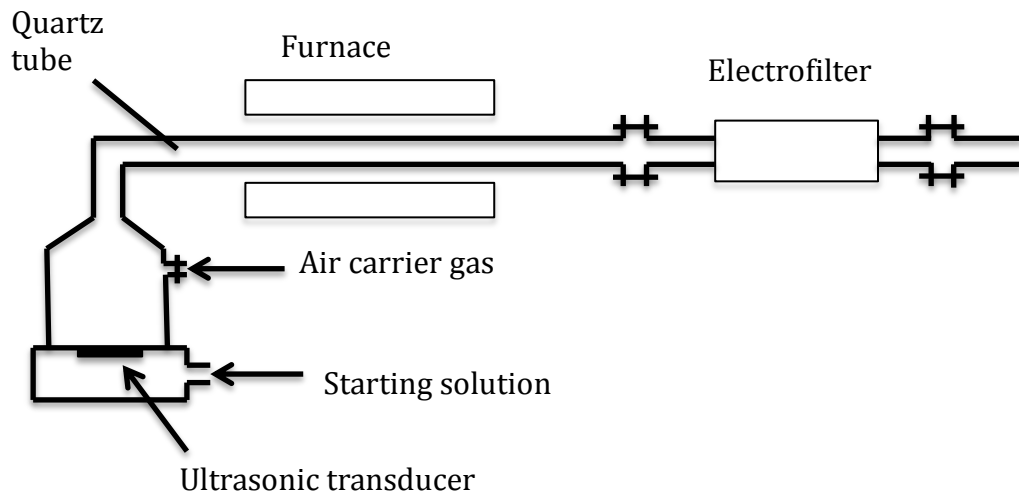

Fig 2.8: Schematic diagram of 3Y-TZP particle preparation apparatus

2.7 Densification of YSZ nanopowders

Densification, or deaerating, refers to removing the porosity from a fine-grained powder to form a robust, bulk, and essentially pore-free material (usually 95–98% of the theoretical density). A powder compact initially has two distinct forms of porosity, inter- and intraparticle porosity, as schematically shown in Figure 2.9. Densification of a fine-grained powder can occur by one of three broad mechanisms: sintering, particle or crystal rearrangement, and plastic deformation [16].
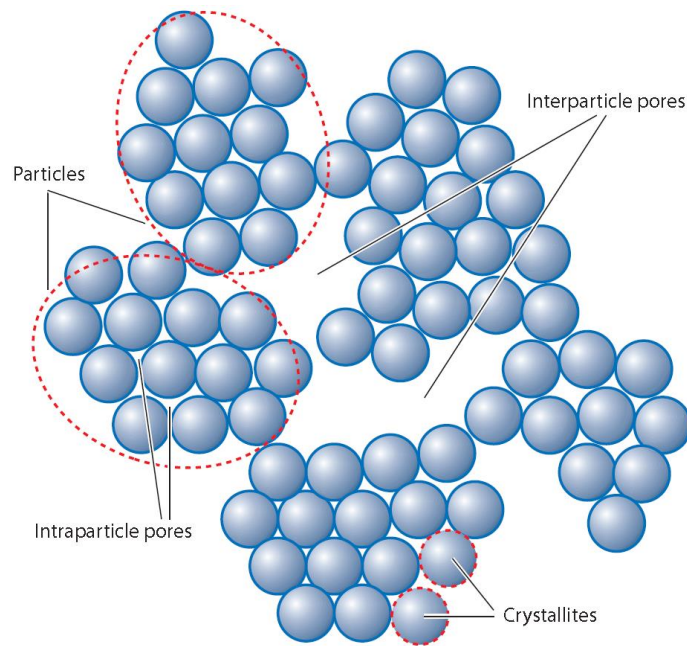

Fig 2.9: schematic of a fine-grained powder illustrating crystallites agglomerated into particles and two distinct types of porosity [16].

Densification as a consequence of the reduction of surface curvature is called sintering, at which the driving force is the reduction of surface energy. The pressure that develops because of surface energy when two particles come together is the so-called sintering pressure or sintering stress. As the particles coalesce by sintering, they form necks through material transport. Figure 2.10 shows the different transport mechanisms. All the mass transport mechanisms depicted contribute to neck formation, but not all cause actual densification. For example, mechanisms 1 and 2 (evaporation and surface diffusion) in Figure 2.10 do not bring the particle centers closer together and therefore do not cause densification; rather, these mechanisms cause particle coarsening. Thus, sintering can be regarded as competition between particle coarsening and densification. To maximize densification, the mass transport mechanisms need to be promoted. High heating rate tend to favor densification over coarsening because surface diffusion has low activation energy and is more active at lower-temperature regimes than grain boundary or volume diffusion. Thus, by quickly bringing the fine-grained powder to the desired temperature, one can minimize coarsening while emphasizing densification [16].
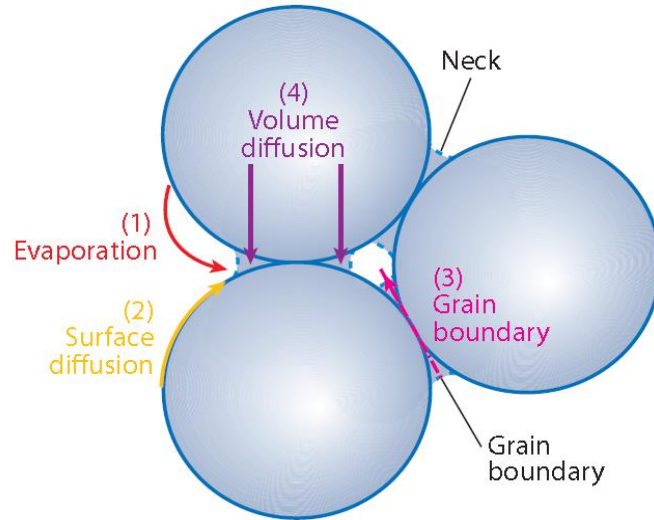
Fig 2.10: Mass transport mechanisms that are involved in sintering [16].
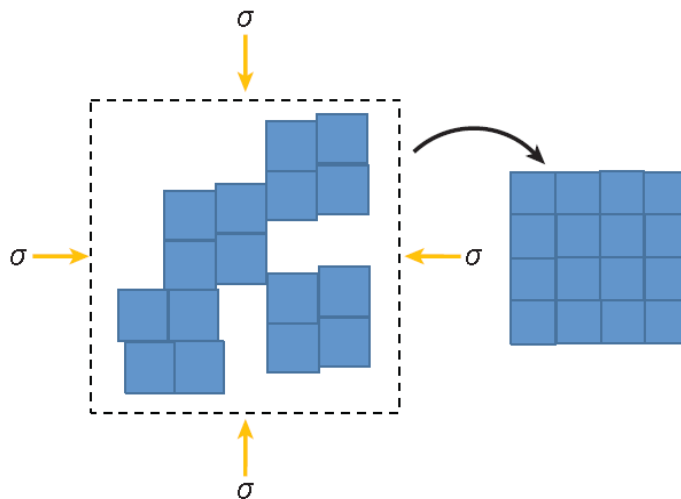

Fig 2.11: Schematic of particle rearrangement mechanism caused by applied pressures [16].

Figure 2.11 shows the schematic of densification based on particle (or crystallite) rearrangement as a result of applied pressure. These mechanisms are temperature activated and should be facilitated by surface diffusion and/or grain boundary diffusion. The third class of possible densification mechanisms is densification caused by plastic deformation. Plastic deformation occurs when the applied stress exceeds the compressive yield stress of the materials, and is expected to occur instantaneously.

Dahl P. et al. [17] studied densification of nanocrystalline yttria stabilized zirconia (YSZ) powder with 8 mol% Y_2O_3 by spark plasma sintering, hot pressing and conventional sintering. The spark plasma sintering technique was shown to be superior to the other methods giving dense materials (>96%) with uniform morphology at lower temperatures and shorter sintering time.

Spark plasma sintering is performed in vacuum using cylindrical graphite dies also working as the heating element. A uniaxial pressure varying from 50 to 110 MPa can be applied at room temperature that should be released at the end of the holding time at the sintering temperature. Hot pressing (HP) is performed under nitrogen flow in a clam furnace using cylindrical graphite dies with an inner diameter of 15 mm. After heating to 600°C, a uniaxial pressure of 25 MPa can be applied before heating to sintering temperature (1150– 1300°C). The pressure should be released after desired sintering time followed by cooling to room temperature. Conventional sintering is performed in air in a muffle furnace.

SPS is shown to be a highly efficient technique for densification of YSZ at temperatures 100–200°C lower than that needed by HP. For HP with an applied pressure of 25 MPa, a

temperature of 1300°C is needed to obtain fully dense (>99% of theoretical value) YSZ materials. In comparison, 1150°C for 5 min (100 MPa) was sufficient when using the SPS technique. The higher pressure used in SPS can partly explain the lower sintering temperature. The main reason for both the short sintering time and reduced temperature, however, is the efficient heat transfer as well as the self-heating from spark discharge between the particles [17].

The other widely used method of densification is the current-activated, pressure-assisted densification (CAPAD), which has two distinct advantages; the efficiency of the process and the unique materials that can be fabricated by it. Because of using high electric currents, CAPAD is capable of densifying powders to full density much faster and at lower temperatures than by traditional methods such as pressureless sintering and hot pressing (HP). For example, a typical CAPAD run is approximately 20 min from start to finish, in contrast to processing times on the order of hours required for conventional methods. Garay J.E. [16] has done an extensive study on the fundamental and practical issues of current-activated, pressure-assisted densification (CAPAD). As shown in figure 2.12(a) and (b), a typical CAPAD apparatus consists of a vacuum chamber, electrodes for both current and load delivery, and a power supply capable of delivering high electric currents at relatively low voltages. The initially powder is densified inside a die that has been placed between the electrodes. Fig 2.13 shows the schematic of the die and the powder system. The most common die and plunger material is high-purity, high-density graphite because graphite has excellent mechanical strength up to very high temperatures, as well as high thermal and electrical conductivity. Typical values of heating rate are

100–600$^{\circ C}$ min^{-1}, and those for pressure are 30–150 MPa in a CAPAD system.
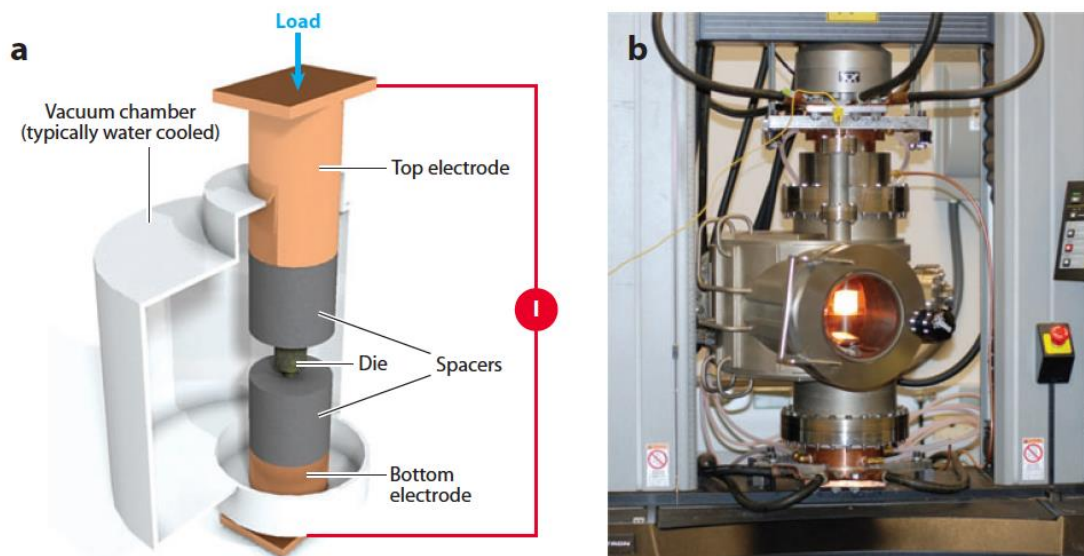

Fig. 2.12: (a) A schematic depicting the main components of a current-activated, pressure-assisted densification (CAPAD) apparatus. (b) A picture of a CAPAD apparatus during an experiment. This particular system was custom built at the University of California, Riverside [16].
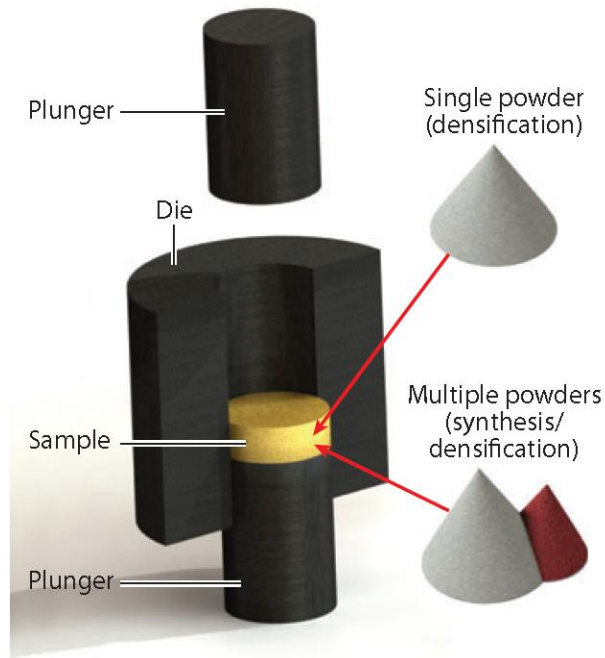
Fig 2.13: Schematic of a die, plungers, and powder. CAPAD can be used for pure densification or for simultaneous synthesis and densification [16].

Refrences

[1] Yuqun X., J. Am. Ceram. Soc., 82 [3] 768–70 (1999).

[2] Jian D., Tinglian W., Zhiyi L., Wuji Cailiao Zuebao, 8 [1] 51–56 (1993).

[3] Agam M. A., Guo Q., Journal of Nanoscience and Nanotechnology 7 (10): 3615–9 (2007).

[4] Vasylkiv O., Sakka Y., J. Am. Ceram. Soc., 84 [11] 2489–94 (2001).

[5] Boutonmet J.H., Kizling J. Stenius Petal Colloids Surf, (5) 209 (1982).

[6] Lee MH., Tai CY., Lu CH., J. Eur Ceram Soc (19):2593–603, (1999).

[7] Tai CY., Lee MH., Lee, Wu YC., Chem Eng Sci 56:2389–98 (2001).

[8] Yang XF., Li WB., Acta Phys – Chim Sin 18(1):5–9 (2002).

[9] Masters K., Spray Drying Handbook, 4th ed. Wiley, New York (1985).

[10] Messing G. L., Zhang S. C., Jayanthi G. V., J. Am. Ceram Soc, 76 [11] 2707-26 (1993).

[11] Eslamian M., Ahmed M., Ashgriz N., Nanotechnology 17 1674–1685, (2006).

[12] Gaudona M., Djurado E., Menzler N.H., Ceramics International 30 2295–2303, (2004).

[13] Nedeljkovic J.M., Saponjic Z.V., Rakocevic Z. , Jokanovic V., Uskokovic D.P., Nanostruct. Mater. 9 125, (1997).

[14] Vallet-Regi M., Rodriguez-Lorenzo L.M., Ragel C.V., Salinas A.J., Gonzalez-Calbet J.M., Solid State Ionics 101–103 197 (1997).

[15] Dubois B., Ruffier D., Odier P., J. Am. Ceram. SOC. 72 [4] 713-15, (1989).

[16] Garay J.E., Annu. Rev. Mater. Res. 40:445–68, (2010).

[17] Dahl P., Kaus I., Zhao Z., Johnsson M., Nygren M., Wiik K., Grande T., Einarsrud M.-A., Ceramics International 33 1603–1610, (2007).

Chapter 3

Experimental Results

3.1 Introduction

In spray pyrolysis a solution of precursors serves as the starting materials. They are misted into droplets that are carried by gas into a hot furnace where they are rapidly heated and decomposed to form a powder. The general schematic of the spray pyrolysis apparatus that has been used for this thesis is shown in Fig. 3.1. Figure 3.2 on the other hand, shows the apparatus that has been used for this thesis. Various potential precursors were investigated and characterized for the preparation of zirconia and yttria stabilized zirconia (YSZ) nanoparticles, the optimum being zirconium (IV) acetylacetonate $(C_5H_7O_2)_4Zr$ and yttrium (III) acetate hydrate $(CH_3CO_2)_3Y.xH_2O$ solved in methanol. Several atomizers including, ultrasonic nebulizer, fuel injector, collison nebulizer, and airbrush were examined to make the droplets. Among these atomizers, collison nebulizer and airbrush were selected to be used throughout the experiments for having higher rate of powder production.

Using nitrogen gas and a vacuum pump, droplets carried into a furnace and decomposed to form a powder there. The produced powder was accumulated on a special filter at the output of the furnace with the aid of the vacuum pump. XRD method was used to analyze the structure of the produced powders and the effect of furnace temperature on size distribution of the powders. After a critical temperature, increasing furnace temperature resulted in the smaller final particles. The final powders were densified using CAPAD technique and Raman Spectroscopy was administered on the final products which verified the tetragonal phase of the densified YSZ.
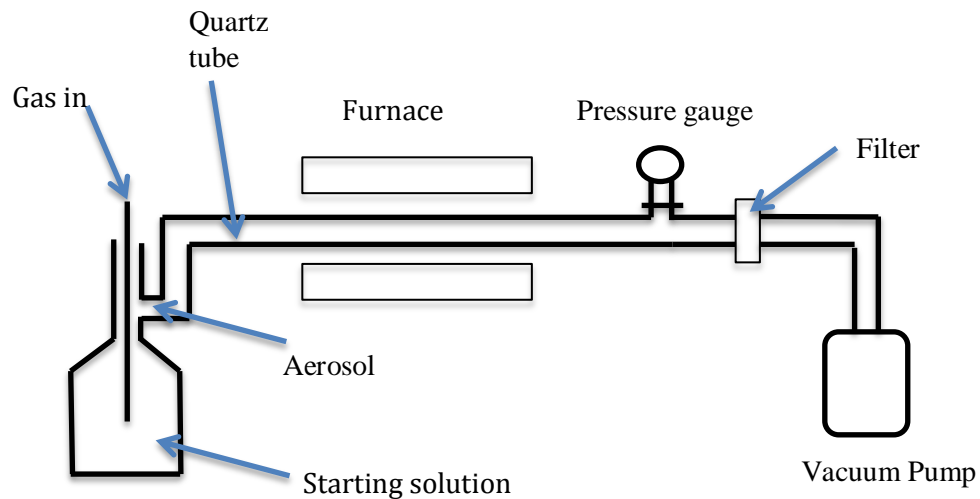
Fig 3.1: schematic diagram of the utilized spray pyrolysis apparatus
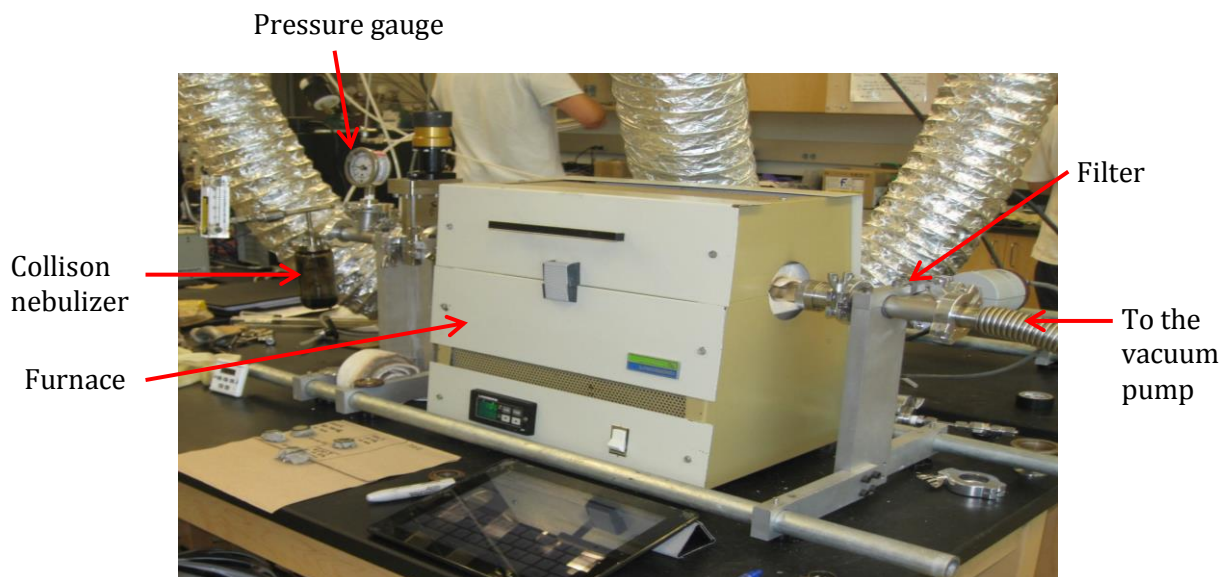
Fig 3.2: SP apparatus for zirconia and YSZ pyrolysis

3.2 Precursor Preparation

The SP experiment of this thesis starts by preparing the precursor to produce pure zirconia. Among several potential solvents for zirconia and YSZ, Methanol was chosen for its good solubility and low cost. Zirconia was solved in methanol using ultrasonic sonicator for 10 minutes. Three parameters were considered in preparing the precursor, volume contribution of zirconium (IV) acetylacetonate, being the main material, volume contribution of methanol as the solvent and the temperature of reaction. The control factors were the solubility of the solvent and sedimentation. Generally, with increasing

the temperature we were able to add more zirconium into the same amount of methanol, but by cooling down the solution to the room temperature the sedimentation became the restricting factor. In order to find the optimum solution, at each step, two of the mentioned parameters kept constant while the other one was changed gradually. At the end, the combination of 5000 mg of Zirconium (IV) acetylacetonate dissolved in 50 mL methanol at room temperature resulted in the best solubility, and no sedimentation observed after 24 hours. The same procedure was followed to prepare ytrrium stabilized zirconia. 6000 mg of Zirconium(IV) acetylacetonate and 218.5 mg of yttrium(III) acetate hydrate were dissolved in 60 mL of methanol to prepare 3YSZ. It gave 3% of molar fraction of yttria to zirconia.

3.3 Atomizers

The theory of operation of atomizers or nebulizers is that when a liquid or a gas is forced through a tube with a constriction, the speed of the liquid or gas is greatest at the constriction and the pressure on the sides of the tube is least at that point. The total energy, which is the sum of kinetic energy of flow and pressure energy, is constant in the tube which can be used to provide suction by forcing water through a constriction. This in turn, leads to creating lateral negative pressure at the jet (Fig 3.3) [1]. Atmospheric

pressure, pushing down on the surface of the water, forces water up the capillary tube. As water leaves the capillary tube, it hits the gas stream and is broken up into an aerosol by the force of gas flow from the jet.
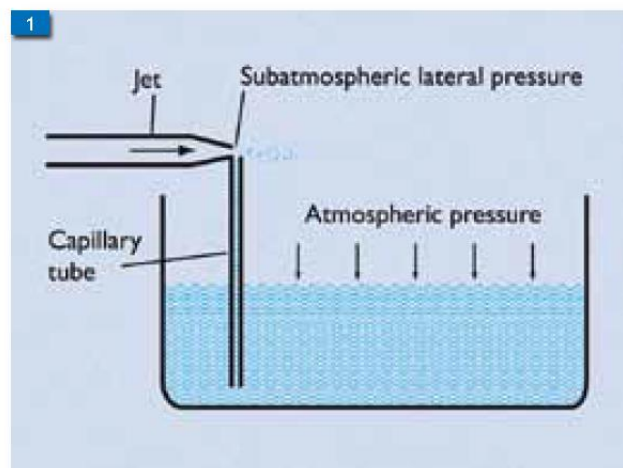

Fig 3.3: Atomization of a liquid in a jet nebulizer

The first atomizer that was utilized in our experiments was a collison nebulizer as can be seen in Fig 3.4. After a few experiments an airbrush atomizer that can be seen in Fig 3.5 and Fig 3.6 replaced it. Even though the main application of the airbrush is in painting, it well suited for our purpose by providing a much higher rate of powder production. Nitrogen gas was used in both atomizers.

a

b

Compressed air in

Aerosol out

Baffle

Spray fluid
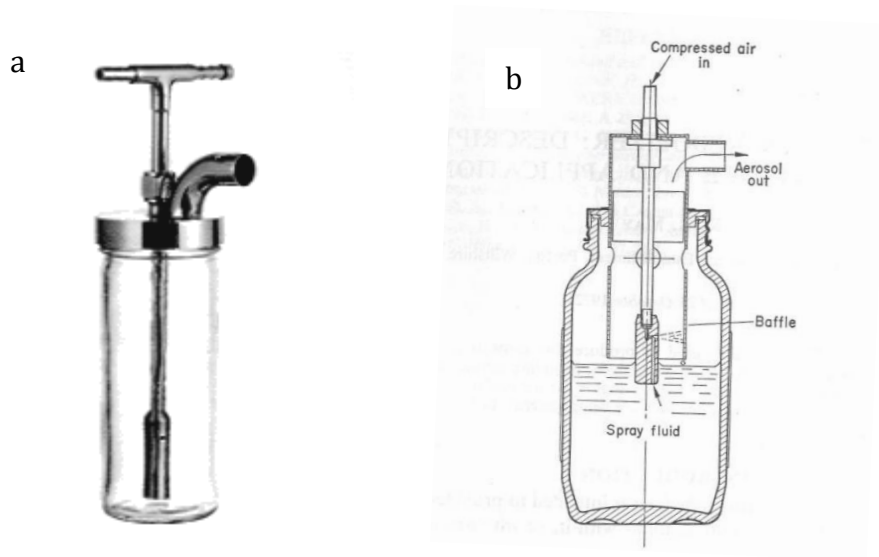
Fig 3.4: (a) and (b) a Collison Nebulizer and its schematic [2],[3]

HP-BCS

Fig 3.5: Iwata eclipse airbrush, model hp-bcs
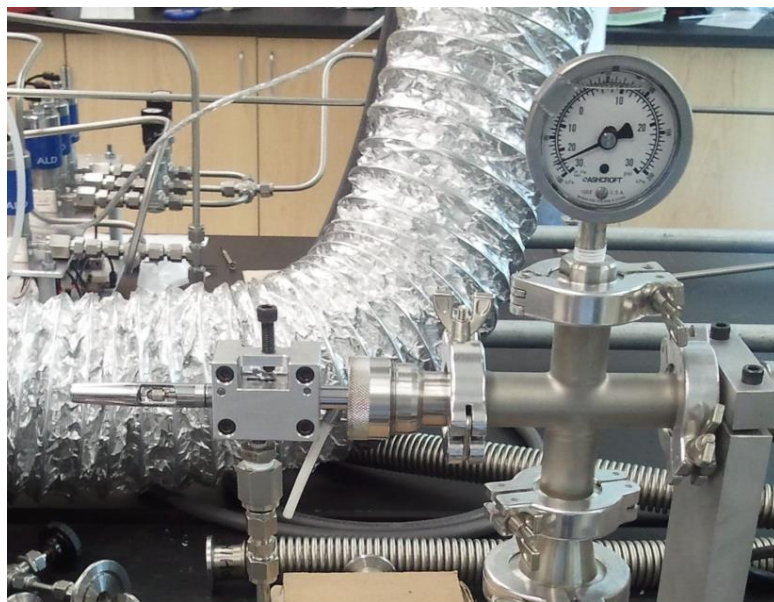
Fig 3.6: airbrush in place for our SP apparatus

3.4 XRD and TEM analysis of the Powders

In order to determine the structural characteristics and phase proportions of the acquired powder, X-Ray Diffraction and Transmission Electron Microscopy (TEM) method was used. The recorded XRD patterns were compared to the reference XRD pattern of zirconium and YSZ powders. The first data analysis was done to determine the effect of the furnace temperature on the produced powders. For this purpose the temperature of furnace varied from 350 °C up to 1000 °C. As can be seen in Figures 3.7-10, after the threshold temperature that was 650 °C for our case, increasing the temperature results in peaks with higher intensity and narrower width, which is a direct consequence of

increment in the grain size. This on the other hand is compensated by the increase in the efficiency of powder synthesis. The XRD pattern below the threshold temperature shows that we were not able to produce zirconium or yttrium stabilized zirconium particles. It is worth mentioning that 950°C and 1000°C resulted in the same XRD patterns. The same procedure was followed in preparing 3YSZ and 6YSZ powders. Figures 3.11-16 and 3.17-19 show the effect of furnace temperature on the produced 3YSZ and 6YSZ powders respectively.

The produced zirconium and YSZ powders were then analyzed using TEM method to get a better understanding of their structural characteristics. Figures 3.20 shows the TEM pictures of Zirconia at furnace temperature of 950°C and Figures 3.21-23 show the TEM images of 3YSZ at furnace temperatures of 650°C, 750°C, and 950°C. As can be seen in Fig 3.20 the produced zirconia has a cubic structure. And Figures 3.21-23 show that the 3YSZ sample has a tetragonal structure.

Scherrer's equation and Williamson Hull plot were used to determine the grain size of 3YSZ particles that yielded a size range of 8-10 nm at furnace temperature of 950 °C.
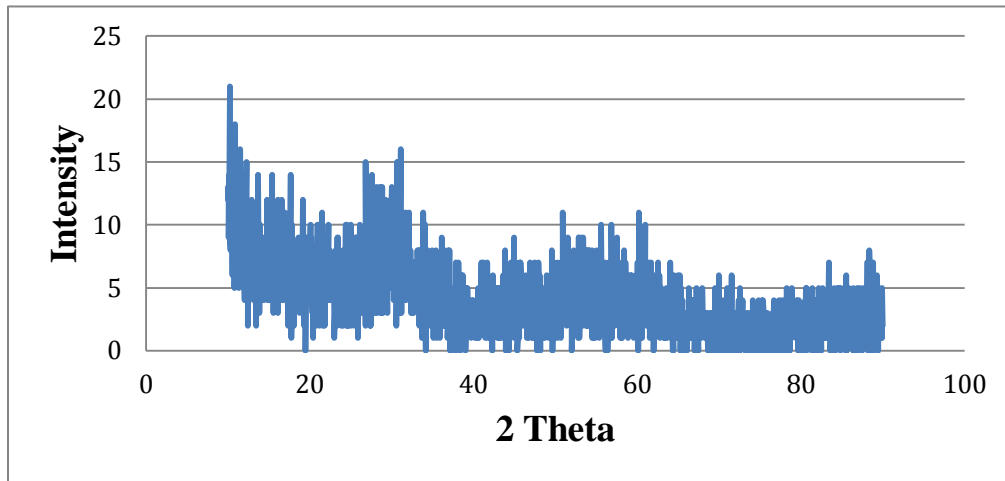
Fig. 3.7: XRD pattern of acquired powder for furnace temperature of 650 °C. Comparing this pattern with the reference pattern for zirconia shows that the acquired powder doesn't contain zirconia.
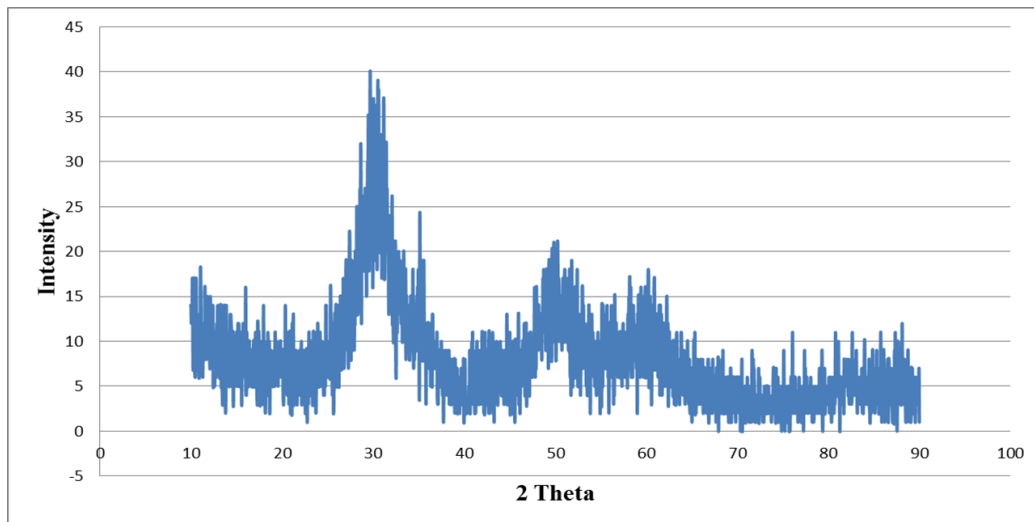
Fig. 3.8: XRD pattern of produced zirconia powder for furnace temperature of 750 °C
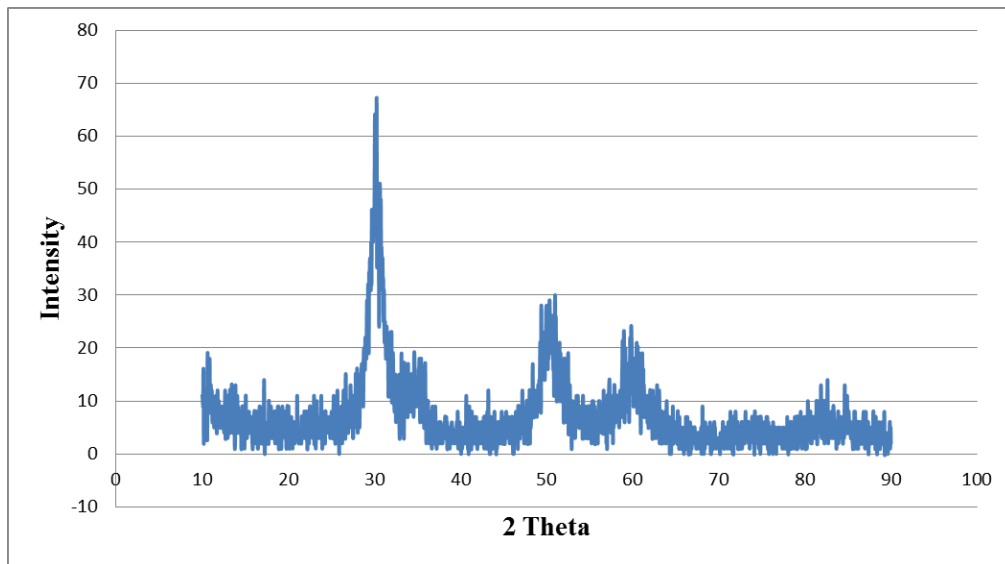
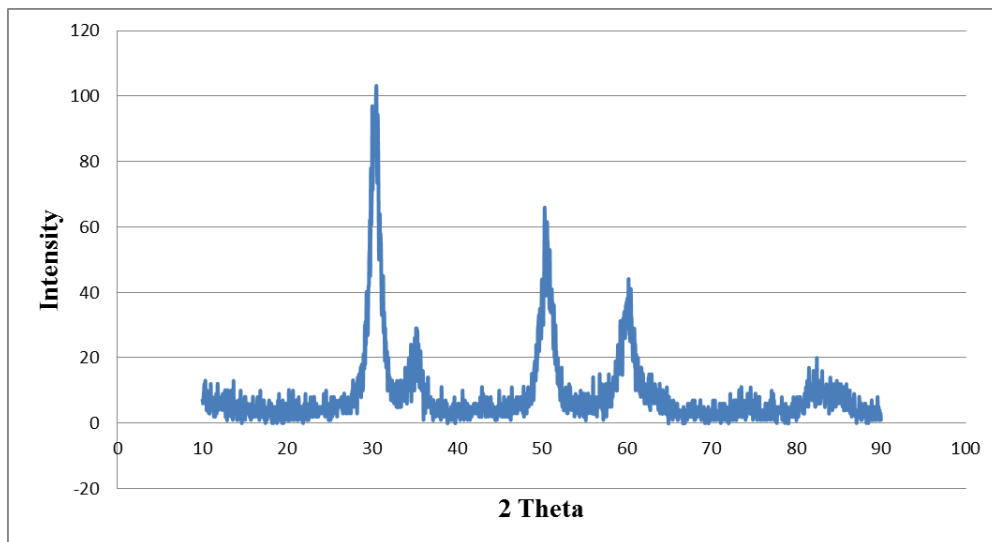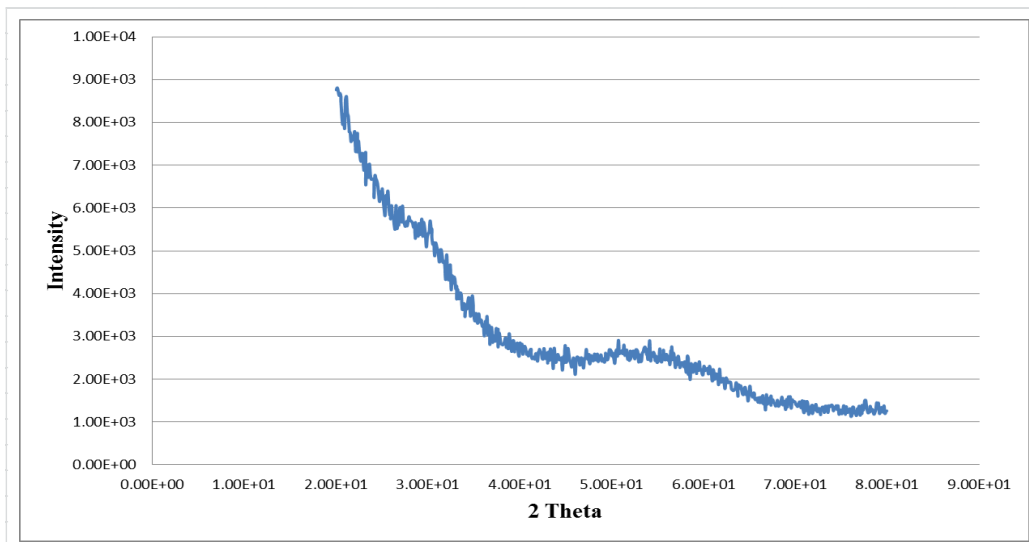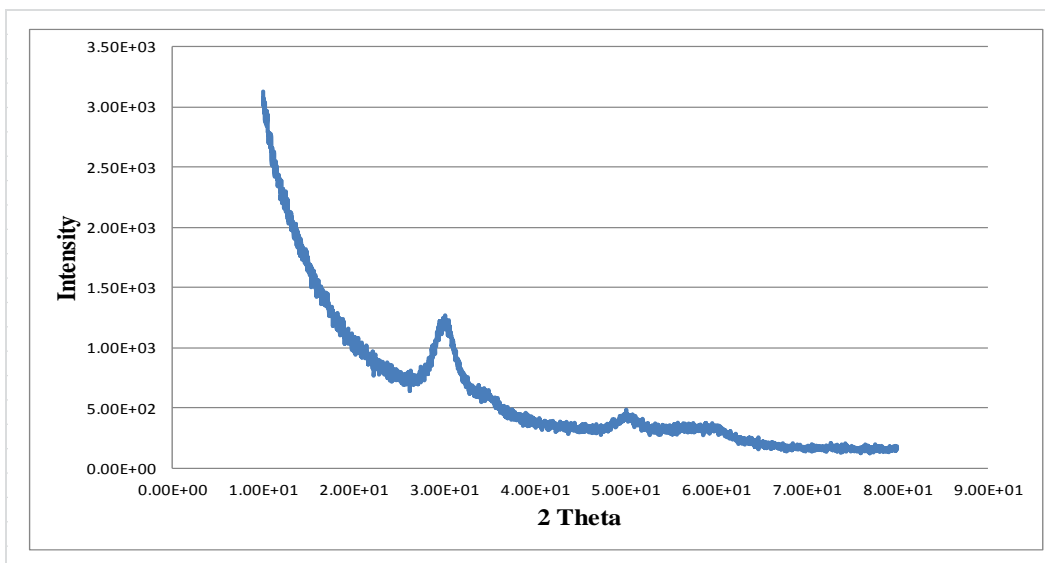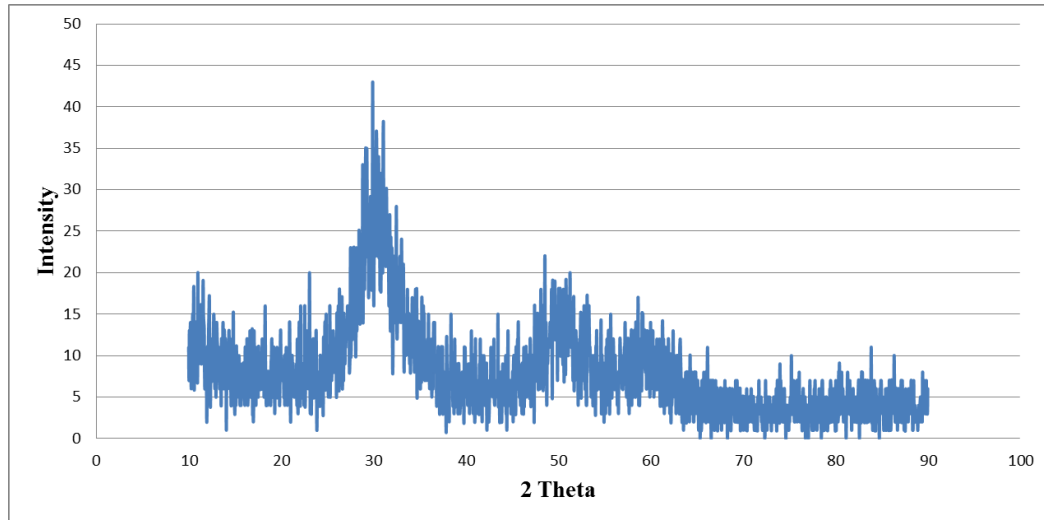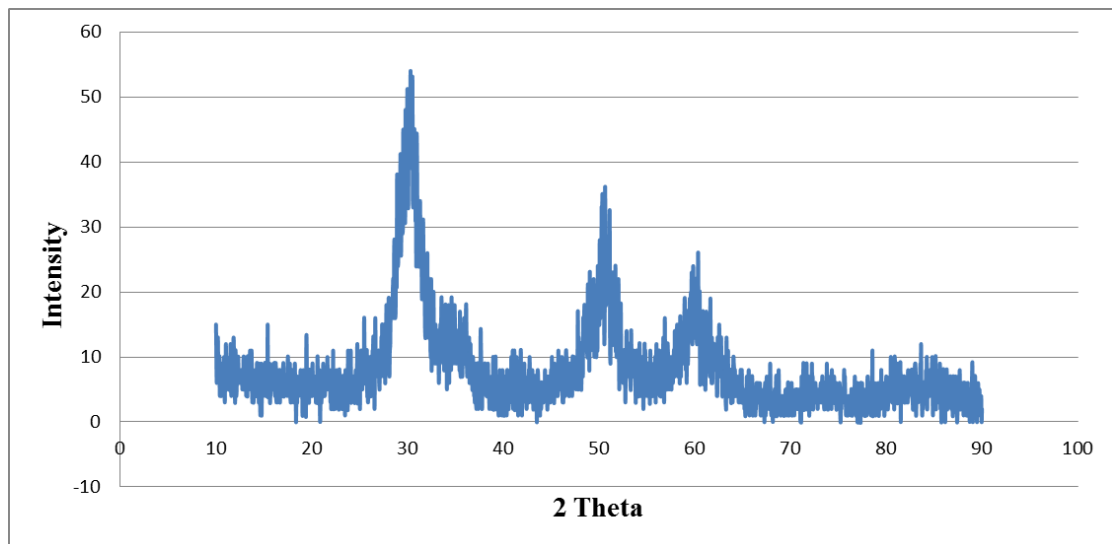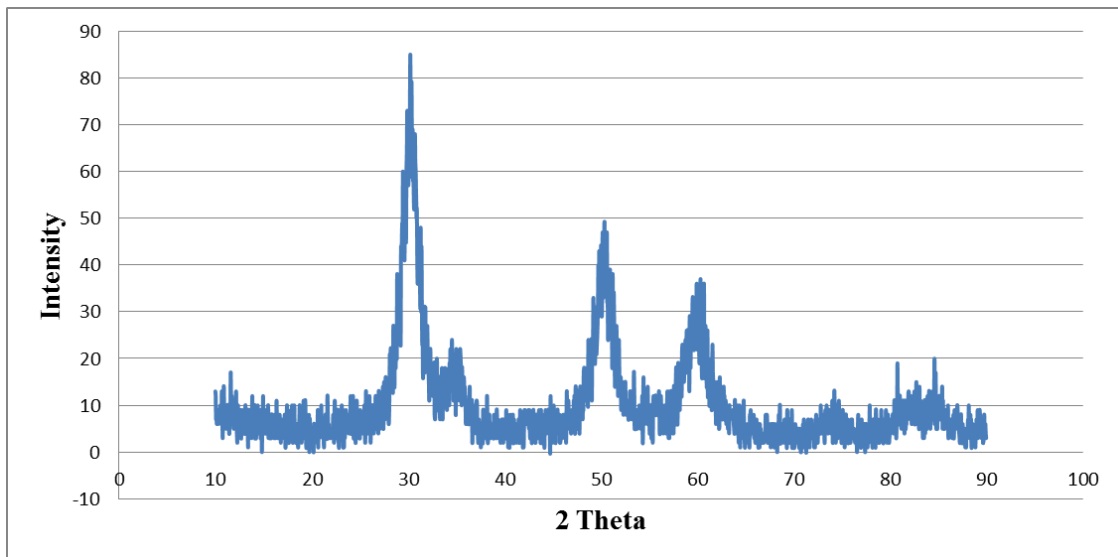Fig. 3.9: XRD pattern of produced zirconia powder for furnace temperature of 850 °C

Fig. 3.10: XRD pattern of produced zirconia powder for furnace temperature of 950 °C

Fig. 3.11: XRD pattern of acquired powder for furnace temperature of 650 °C. Comparing this pattern with the reference pattern for YSZ shows that the acquired powder doesn't contain yttrium stabilized zirconium.

Fig. 3.12: XRD pattern of produced 3YSZ powder for furnace temperature of 700 °C

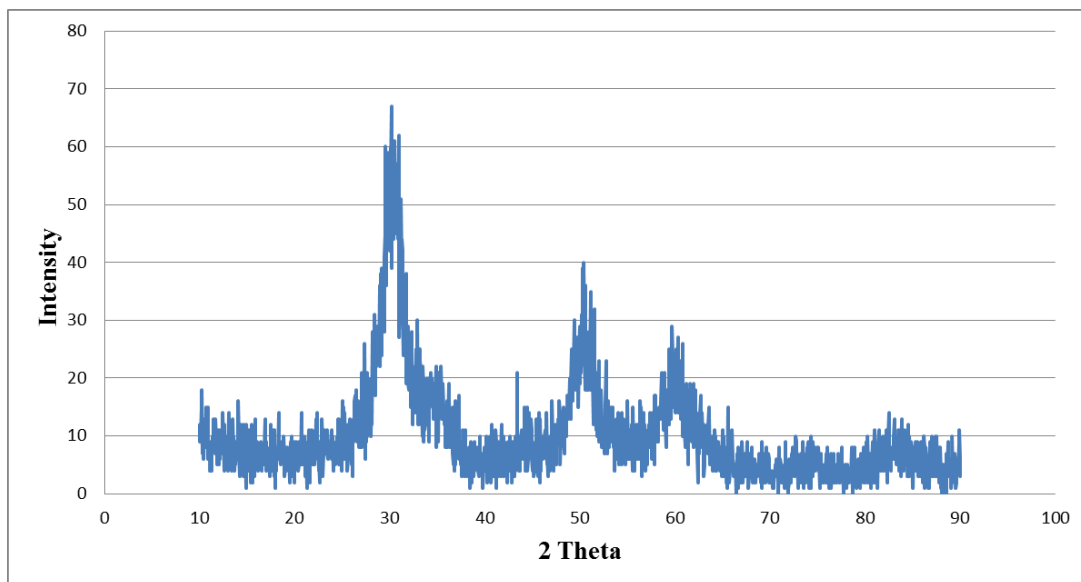Fig. 3.13: XRD pattern of produced 3YSZ powder for furnace temperature of 750 °C

Fig. 3.14: XRD pattern of produced 3YSZ powder for furnace temperature of 850 °C

Fig. 3.15: XRD pattern of produced 3YSZ powder for furnace temperature of 950 °C

Fig. 3.16: XRD pattern of produced 3YSZ powder for furnace temperature of 1000 °C
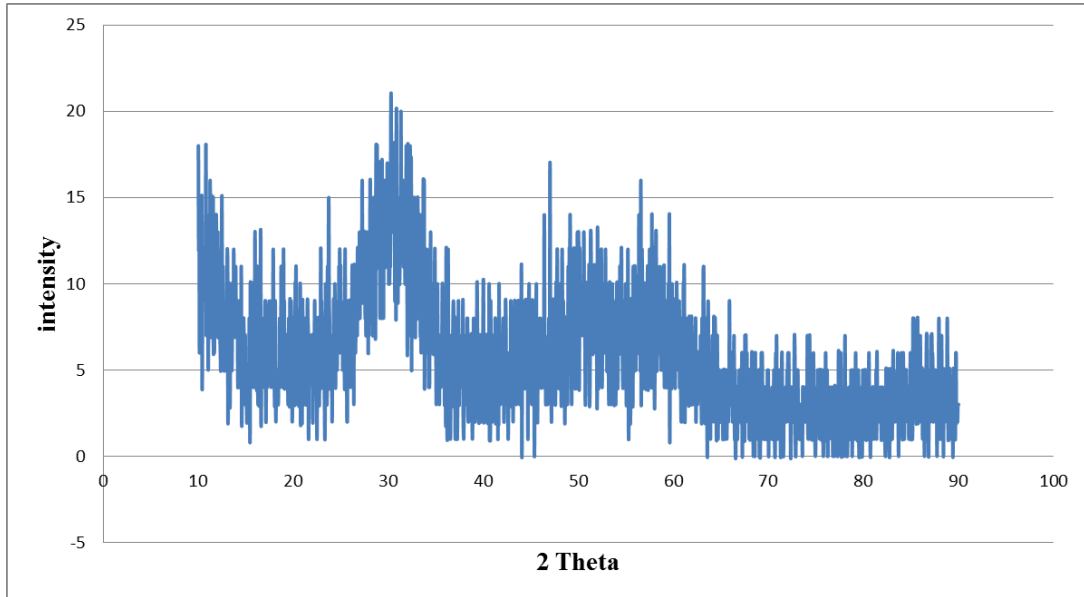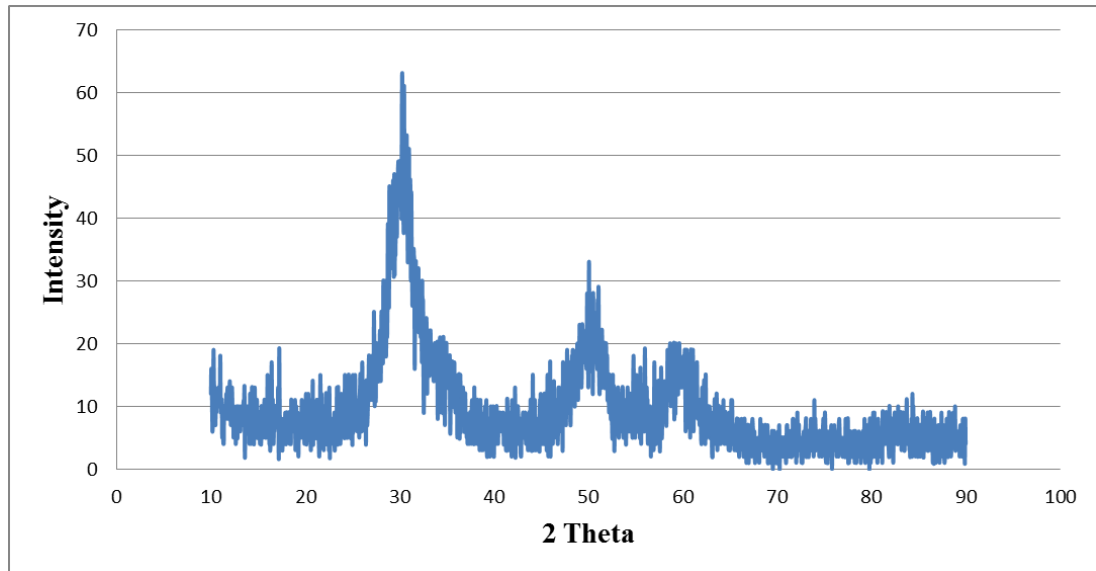
Fig. 3.17: XRD pattern of produced 6YSZ powder for furnace temperature of 750 °C

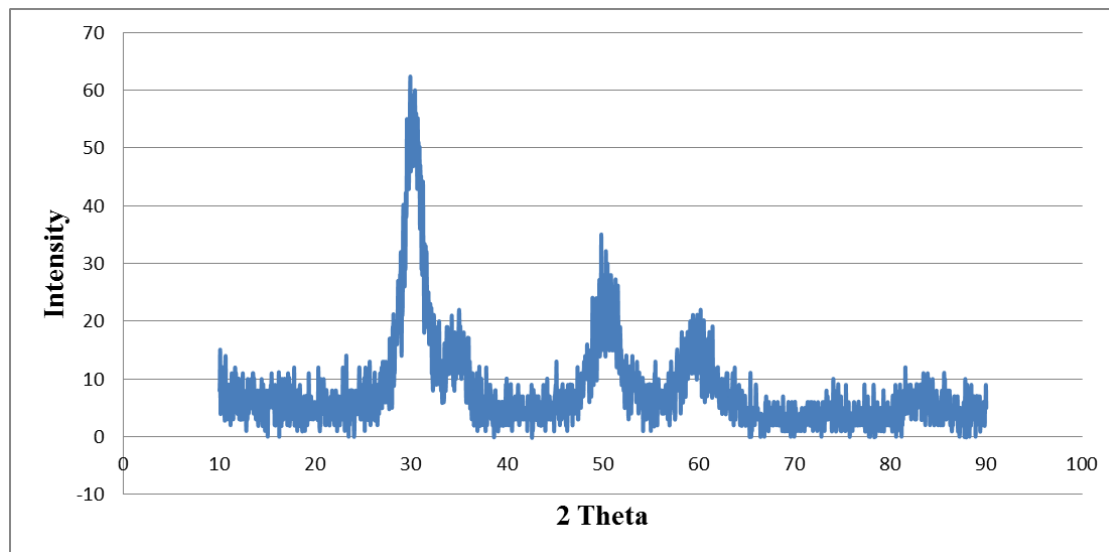Fig. 3.18: XRD pattern of produced 6YSZ powder for furnace temperature of 850 °C

Fig. 3.19: XRD pattern of produced 6YSZ powder for furnace temperature of 950 °C

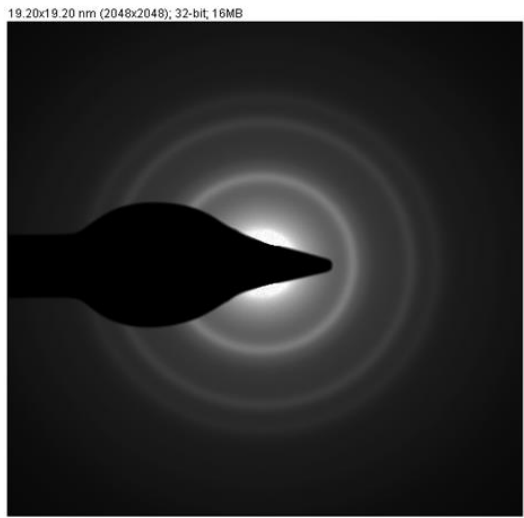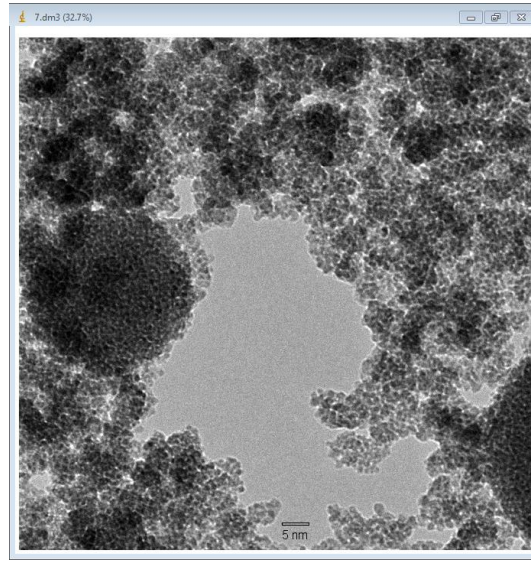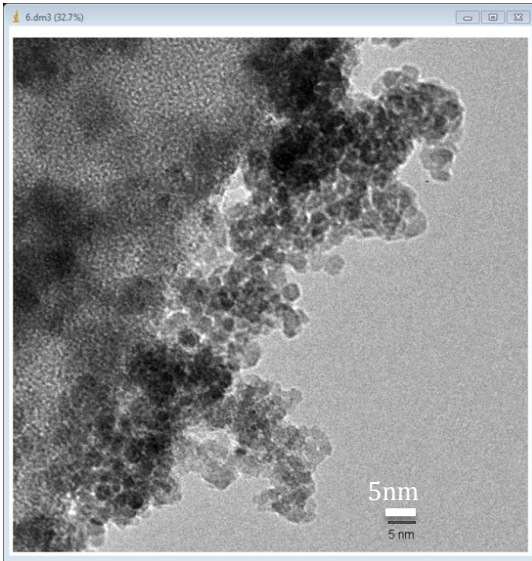19.20x19.20 nm (2048x2048); 32-bit; 16MB

Fig. 3.20: TEM results of the produced pure zirconia for furnace temperature at 950 °C
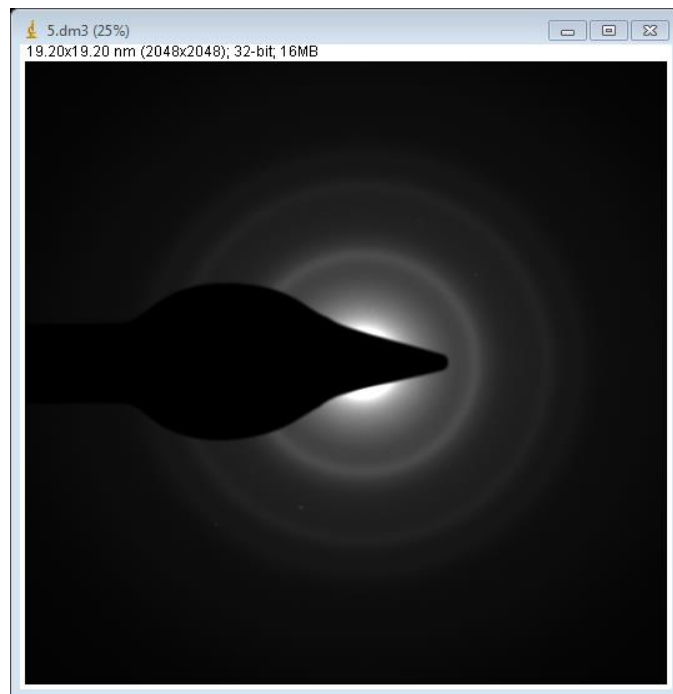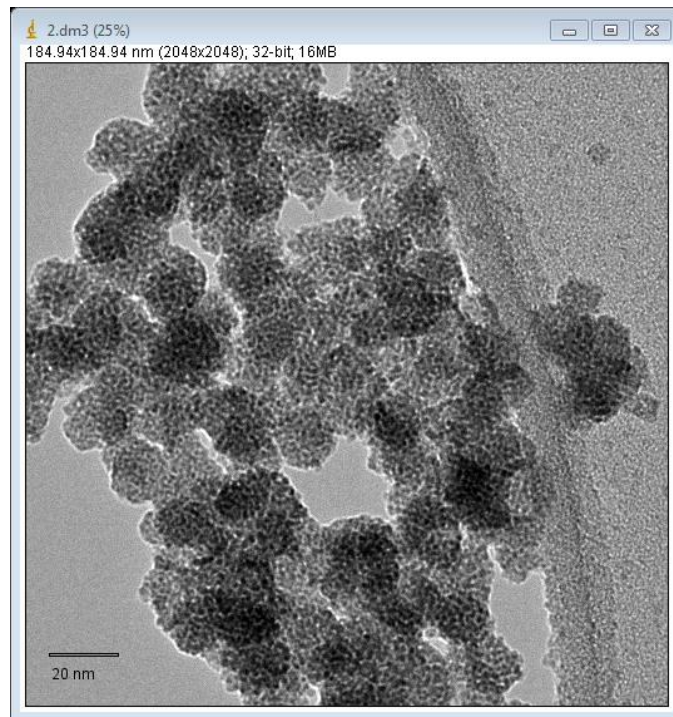
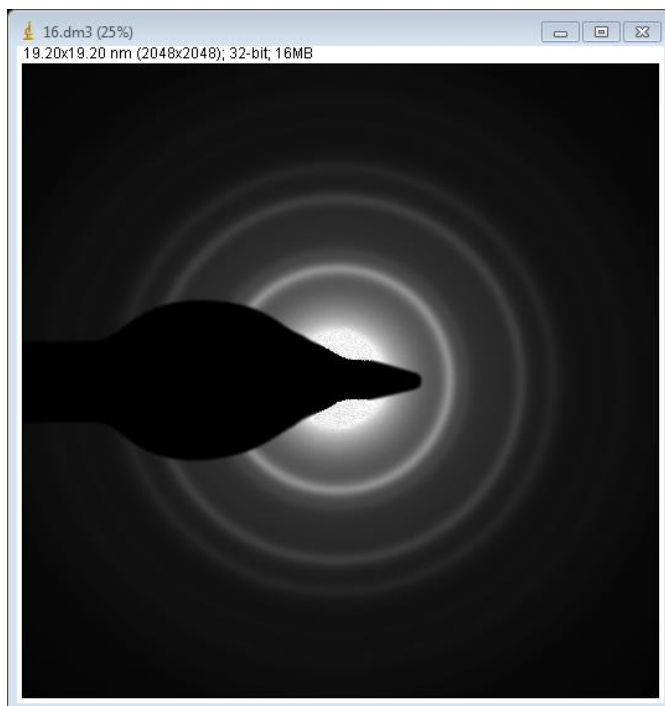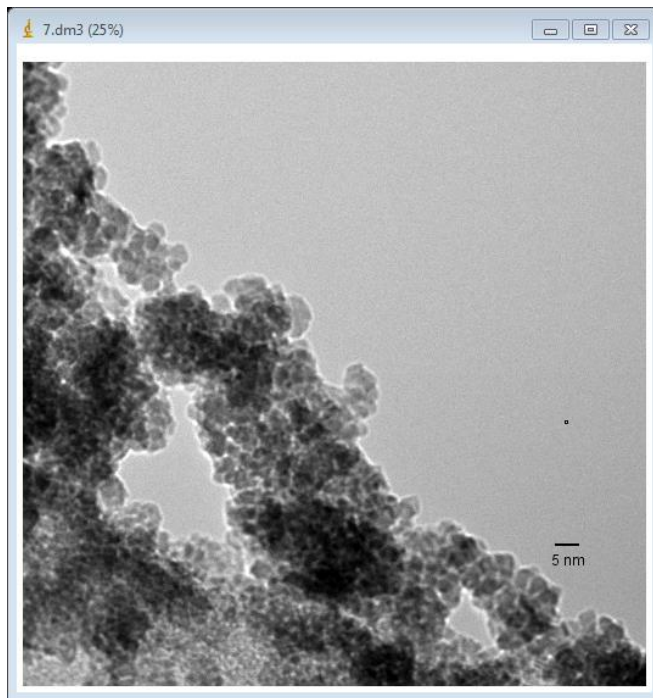Fig. 3.21: TEM results of produced 3YSZ for furnace temperature at 650 °C

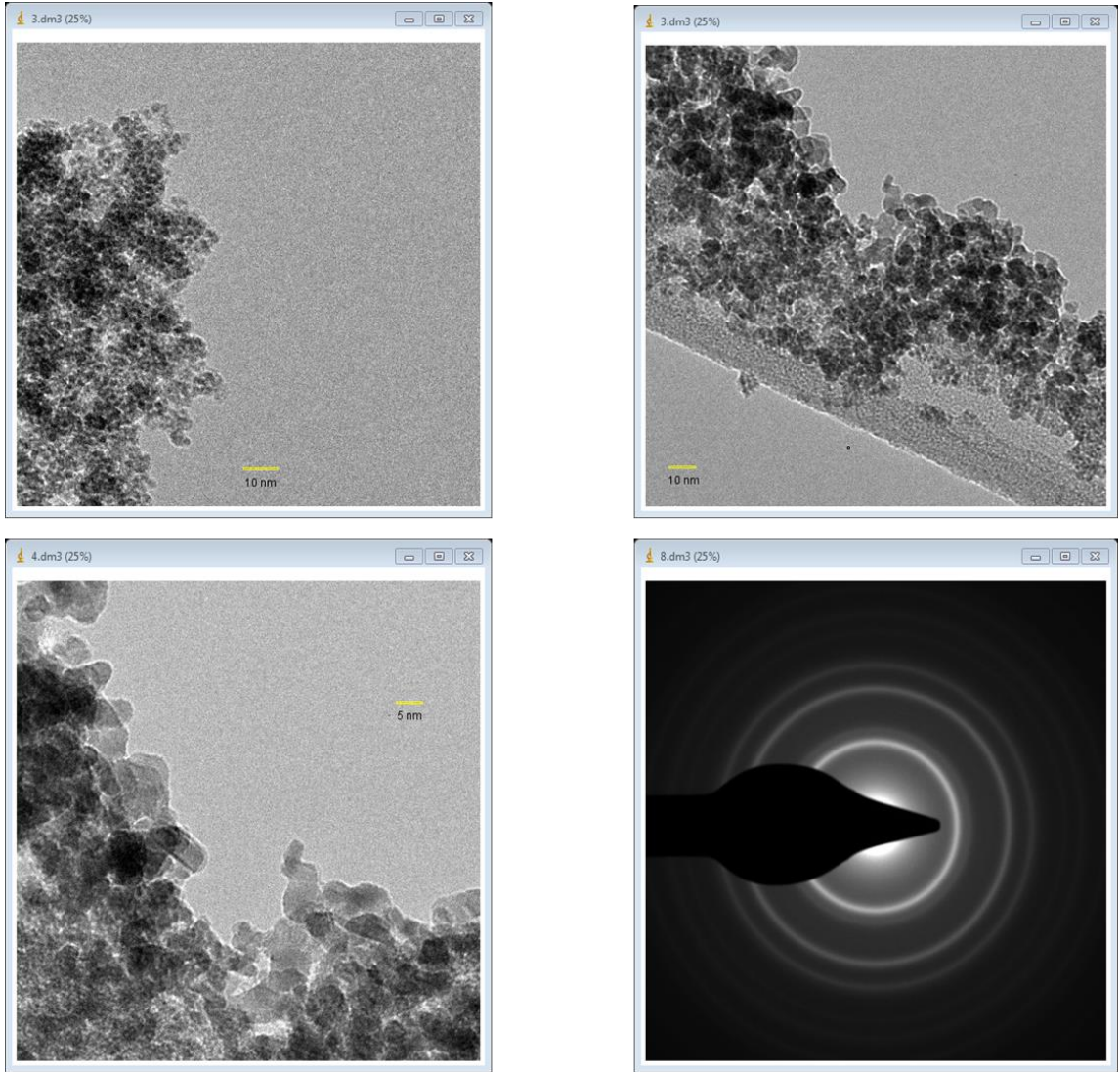Fig. 3.22: TEM results of produced 3YSZ for furnace temperature at 750 °C

Fig. 3.23: TEM results of produced 3YSZ for furnace temperature at 950 °C

3.5 Densification of YSZ and Characterization

The produced 3YSZ powders at furnace temperature of 950°C were then densified using the CAPAD method in Professor Garay's lab at UC, Riverside. Two sets of experiments with different control parameters were examined to run the densification. For the first experiment, pressure of 104 MPa or 30 KN, temperature of 1200°C, 2400 Amp Electrodes, Outgas temperature of 200°C before processing and final outgas temperature of 245 °C at 2.2 eV were selected for the CAPAD densifier. These conditions yielded a 0.68 mm thick densified coin with 61% density from 612mg 3YSZ powder. Dry weight of the sample was 0.4375 grams and its wet weight was 0.3218 g. The XRD results of the densified sample can be seen at Fig 3.24. Fig 3.25 shows the reference XRD pattern for the densified 3YSZ. These two patterns are in a good agreement. In order to determine the structure of the densified sample, its XRD pattern is compared to the one from cubic, monoclinic, and tetragonal 3YSZ. Figure 3.26 demonstrates this comparison and shows that the produced 3YSZ powder and the densified sample have tetragonal structure. This was then confirmed with the results of Raman Spectroscopy and SEM images. As can be seen in Figure 3.26, there are not any peaks indicative of a secondary phase or contamination and there is not any evidence of monoclinic phase. At this dopant level one would normally expect a mixed phase composition. Furthermore, SEM/EDS analysis has been done to confirm the 3% molar level of Yttrium.
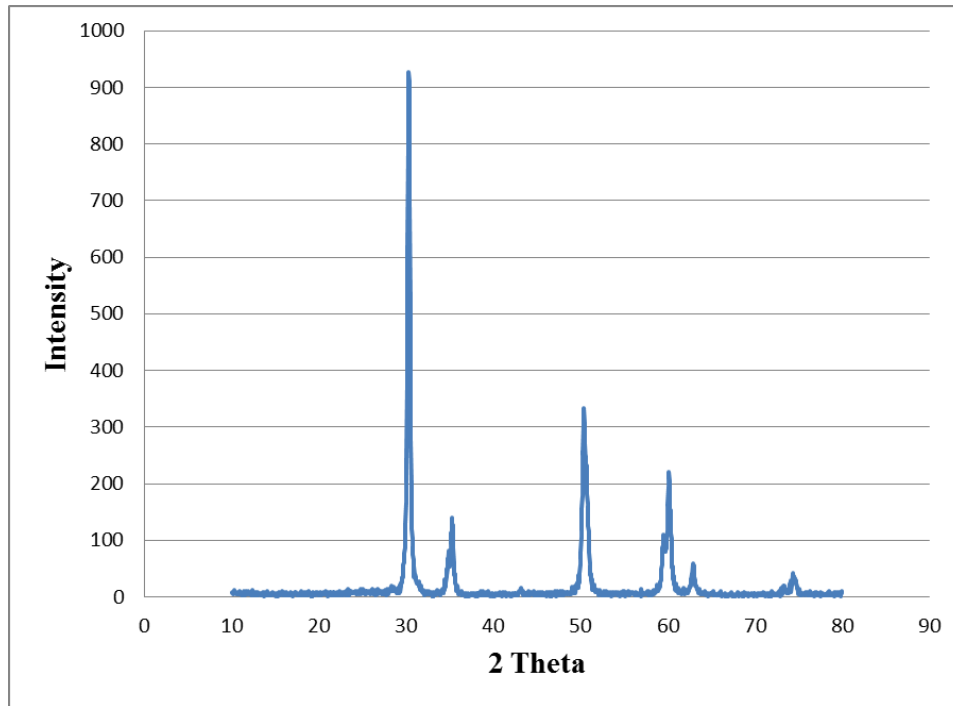
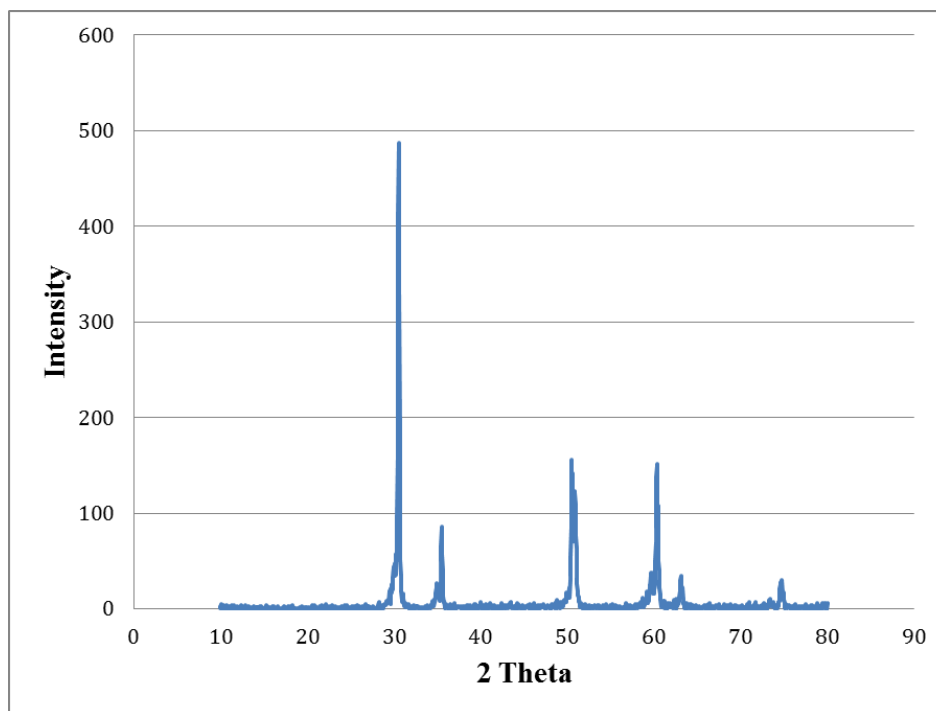Fig 3.24: XRD pattern of the first densified 3YSZ at 1200 °C

Fig 3.25: XRD pattern of the reference densified 3YSZ
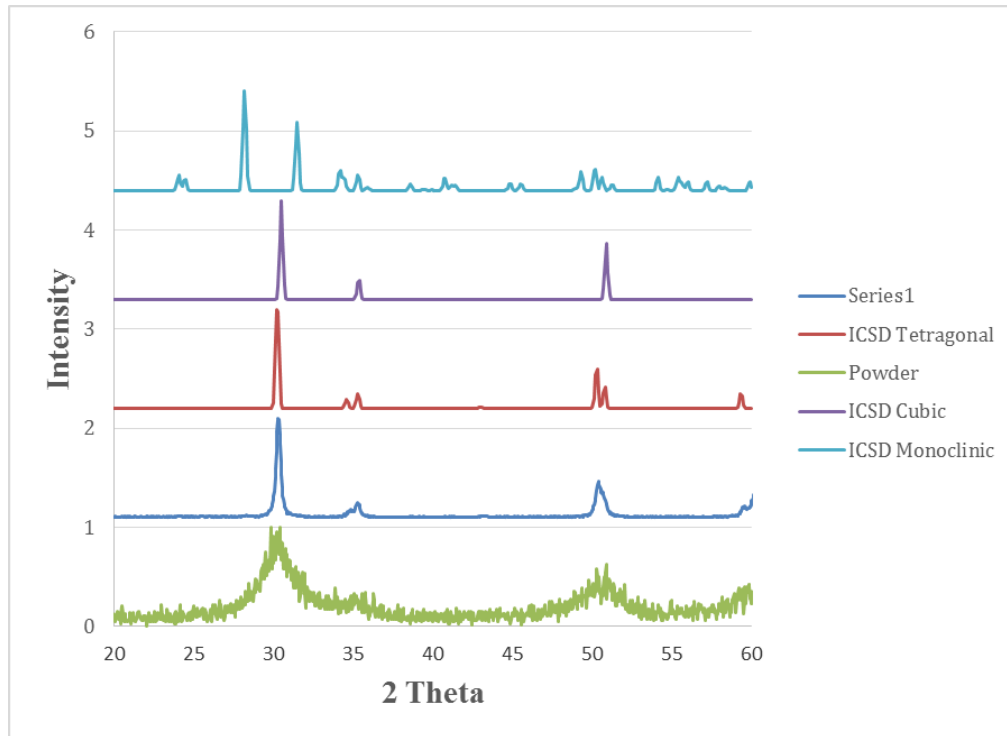
Fig 3.26: XRD patterns for 3YSZ powder (Powder), densified 3YSZ sample at 1200°C (series 1), reference cubic 3YSZ (ICSD Cubic), reference tetragonal 3YSZ (ICSD tetragonal), and reference monoclinic 3YSZ (ICSD Monoclinic).

Figure 3.27 shows the Raman spectra of our densified 3YSZ sample that can be compared to the reference spectra of monoclinic zirconia, cubic, and tetragonal ytrrium stabilized zirconium in Fig 3.28 [4]. In addition to this qualitative comparison, Figure 3.29 shows the wavenumbers associated with each peak at Raman spectra of our sample that can be compared to the data at Table 3.1 [4]. This table provides the wave numbers for Raman peaks of typical monoclinic, cubic, and tetragonal YSZ. These comparisons clearly show that the densified 3YSZ has a tetragonal phase.

Fig 3.27: Raman spectra of the densified 3YSZ at 1200 °C
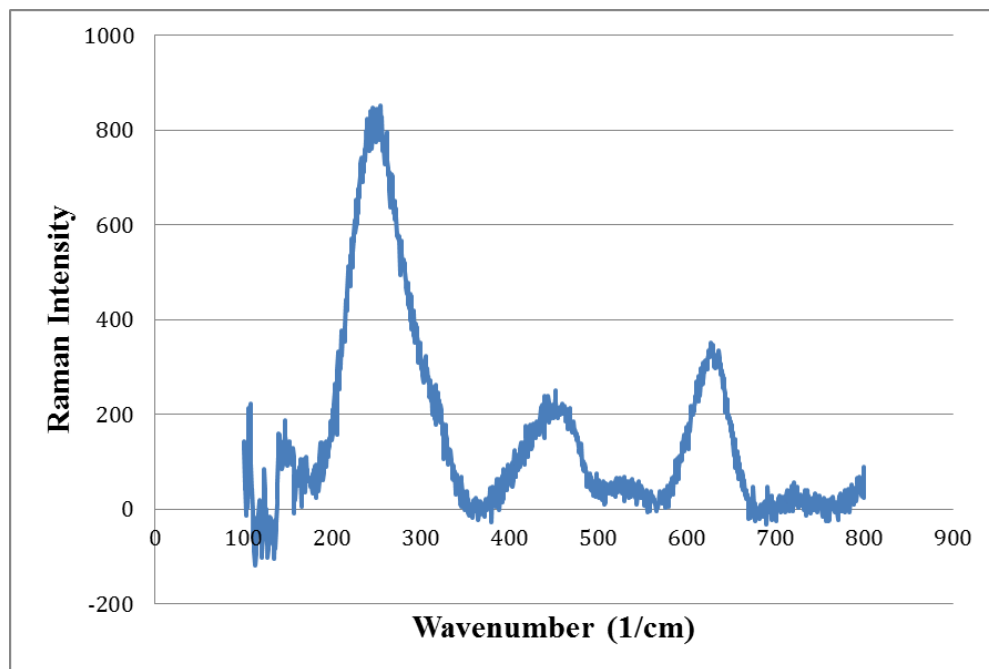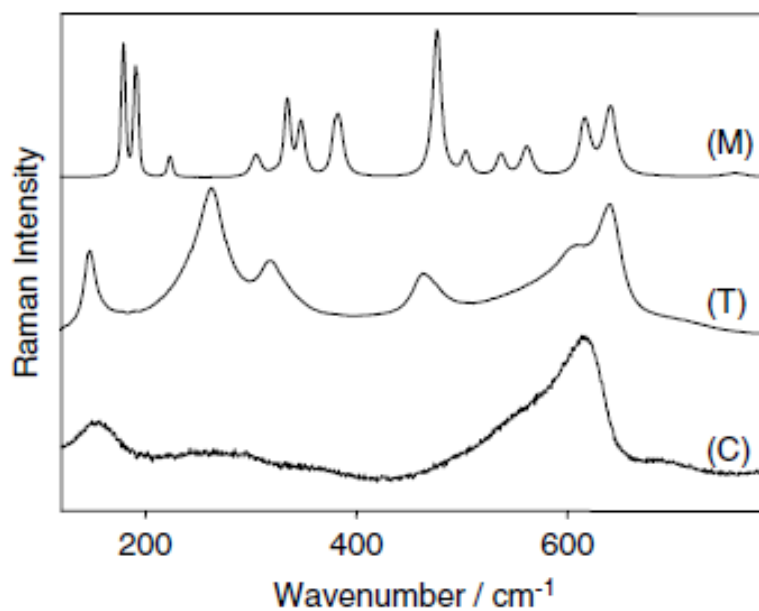

Fig 3.28: Raman spectra of monoclinic (M) ZrO_2, and of typical tetragonal (T) and cubic (C) yttria- stabilized zirconia. Spectral intensities have been normalized to their maximum value.

65
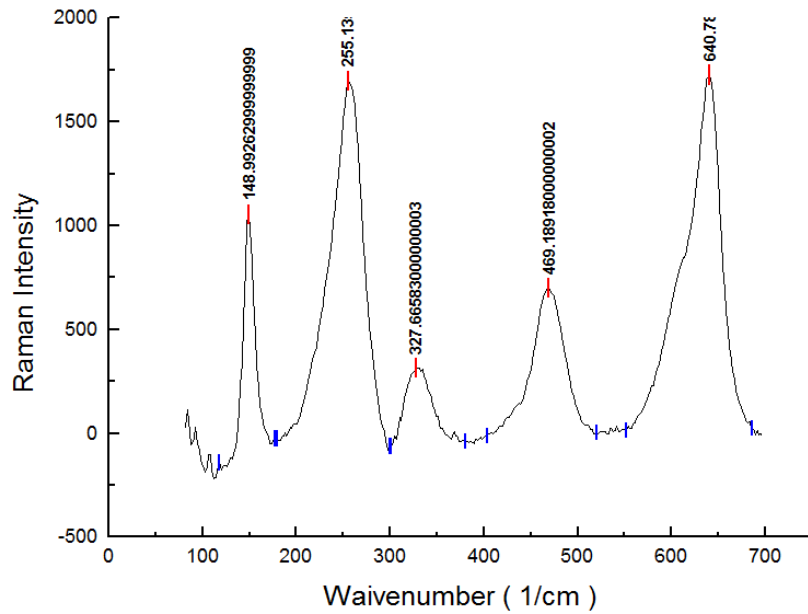
Fig 3.29: wavenumbers associated with each peak at Raman spectra of the densified 3YSZ at 1200 °C

Table 3.1: wave numbers corresponding to the Raman peaks at typical monoclinic, cubic, and tetragonal YSZ spectra. (peak intensities: w=weak; m = medium; s = strong; b = broad)

Monoclinic (cm^{-1})	Tetragonal (cm^{-1})	Cubic (cm^{-1})
97 (m)	–	155 (m)
179 (s)	147 (m)	–
191 (s)	–	–
223 (w)	261 (s)	278 (w, b)
305 (w)	318 (m)	–
333 (m)	–	–
347 (m)	–	367 (w, b)
381 (m)	–	–
475 (s)	463 (m)	–
504 (w)	–	–
537 (w)	–	–
560 (w)	–	579 (m, b)
616 (m)	611 (m)	617 (s, b)
640 (m)	641 (s)	–

In order to further characterize the densified sample, SEM/EDS technique was used to determine the molar contribution of ytrrium to our densified sample. Fig 3.30 shows the EDS spectra of the densified 3% YSZ; the contributed elements can be found in Table 3.2. By comparing the elements and their atomic fractions in our sample with those of the reference 3YSZ (Table 3.3) we confirmed that the densified powder had 3% ytrrium in it and there was not any impurity in our sample. Figure 3.31 and 3.32 show the SEM images of the densified sample with scale bar equal to 200nm.
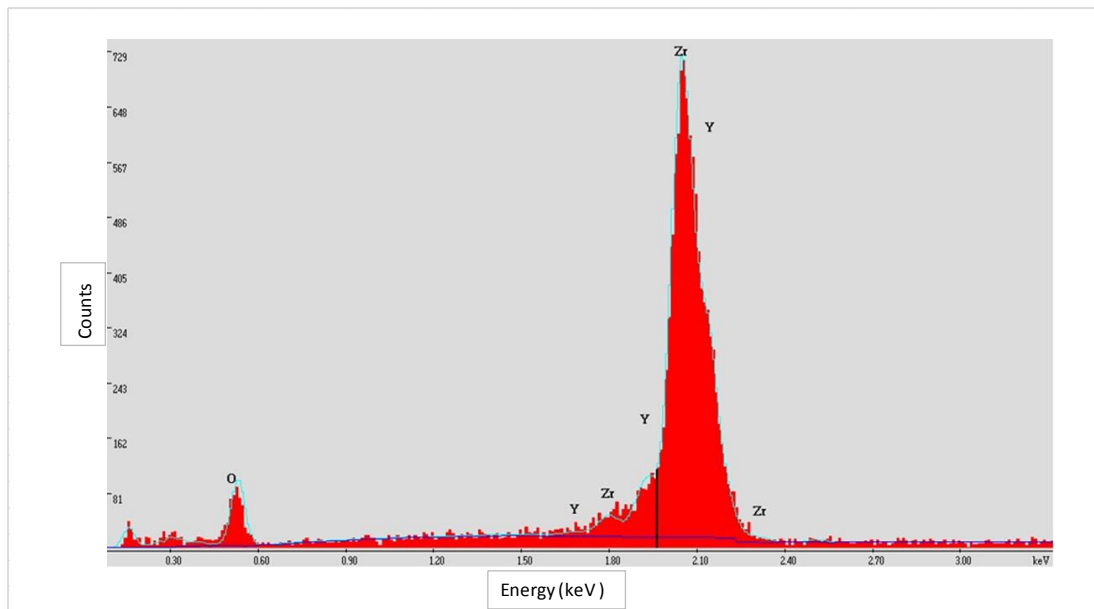

Fig 3.30: EDS spectra of the densified 3% YSZ

Table 3.3: Components of reference 3YSZ sample by

Table 3.2: Components of our 3% YSZ sample by EDS/SEM

Acquisitio Date: 4-Feb-2013			
EDAX ZAF Standardl			
Element Normalized			
SEC Table : Default			
Element	Wt %	At %	K-Ratio
O K	18.72	56.71	0.0663
Y L	7.15	3.9	0.0661
ZrL	74.13	39.39	0.69
Total	100	100	

Element	Net Inte.	Bkgd Inte	Inte. Erro	P/B
O K	21.7	0.8	4.97	27.13
Y L	8.32	3.15	10.28	2.64
ZrL	81.3	3.1	2.57	26.23

Acquisitio Date:22-Feb-2013			
EDAX ZAF Standardl			
Element Normalized			
SEC Table : Default			
Element	Wt %	At %	K-Ratio
O K	18.96	57.09	0.0302
Y L	7.79	4.22	0.0719
ZrL	73.25	38.69	0.6935
Total	100	100	

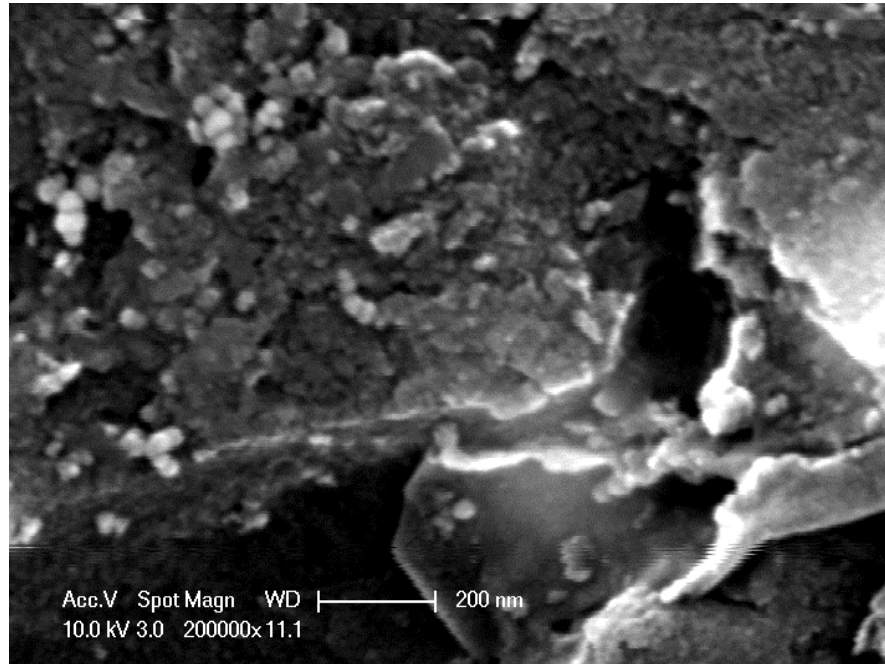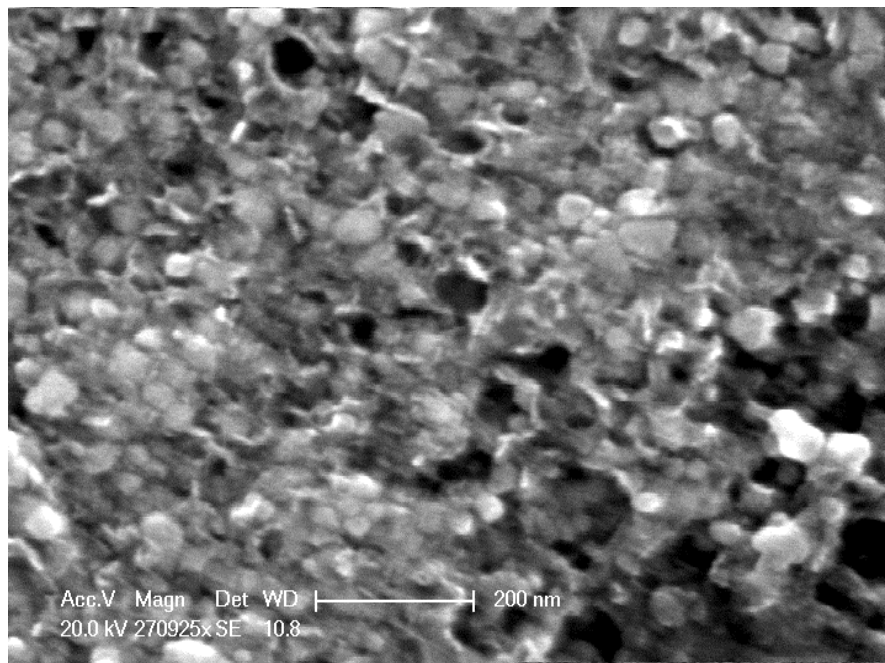| Element	Net Inte.	Bkgd Inte	Inte. Erro	P/B
O K	20.13	0.61	5.18	33
Y L	26.91	6.86	5.34	3.92
ZrL	252.26	6.81	1.46	37.04

Fig 3.31: SEM image of the densified 3YSZ

Fig 3.32: SEM image of the densified 3YSZ

The only downside of the densified sample at the first experiment was that its density (61%) was too low. The hypothesis was that the desorption of gasses (water vapor) from the surface had been detrimental to the densification process, thus in the second experiment the powder was baked at 550 °C for 3.5 hours before being densified. TEM results of the 3YSZ powder baked at 550 °C (Fig. 3.33) showed no difference with that of the ones before baking (Fig 3.23). The powder was then transferred to the densification set up as quickly as possible. The other parameter that we changed was the increment of temperature from 1200°C to 1400°C. In the second experiment, we started with 0.4475 gram 3YSZ powder. The densified sample had dry weight of 0.0810 g and wet weight of 0.0689 grams. This yielded in 99.999% density using Archimedes method.

Since the ultimate application of our pyrolyzed YSZ is in the human skull implant for improved optical coherence tomography (OCT) imaging, further modifications should be made on the densified sample to make it transparent to the visible light.

In order to introduce transparency, the densified 3YSZ sample was annealed by placing it in a furnace for 24 hours at 700 °C and then cooling it down at room temperature for.

J.E. Garay et al. [5] have done an intensive research on the factors affecting the transparency of densified YSZ nanoparticles. Their measurements of absorption coefficients and transmission associated with visible light spectrum shows a high peak of absorption at 470 nm. They further analyzed three factors that could potentially be responsible for the 470 nm absorption band, including colloidal metal formation due to either thermal or electrochemical reduction, absorption at grain boundaries, and point defects.

They proceeded by excluding the first possibility, large metal formation, as they did not observe a loss of optical resolution, which would have been expected if they had any large agglomerates of metal in their sample. The second possibility was also rejected because their measured absorption coefficient of their nanocrystalline samples were very similar to those that Savoini et al. [6] have reported for single YSZ crystals, which suggests that grain boundaries do not intrinsically affect the optical properties of YSZ. A much more likely case was that the 470 nm band was a result of point defects. The vacuum in combination with the graphite die at high temperatures of the densification process creates a highly reducing atmosphere leading to oxygen vacancies in the yttria-stabilized zirconia. Their research shows that the dominant absorption centers are oxygen vacancies associated with a free electron. The process of annealing reoxidized their samples and as the time of annealing increased, the optical transparency increased on their samples.

They further expanded their rationale about the insignificant effect of grain boundaries on the optical transparency by analyzing the surface charge layer. The grain boundaries are positively charged because they are dominantly composed of cations. In order to maintain the charge neutrality, a negatively charged surface charge layer surrounds the grain boundaries. Since oxygen vacancies are positively charged the surface charge layer has a low concentration of oxygen vacancies, which confirms the inferior effect of the grain boundaries on the absorption coefficient.

In conclusion, Annealing at 700°C oxidizes the sample, which in turn reduce the absorption. Figure 3.34 shows the densified sample without annealing. As you can see in Figure 3.35, after annealing light can be seen at the other side of the sample.

Comparing the XRD results of the annealed 3YSZ sample (Fig 3.34) with the results of the one without annealing from the second experiment (Fig 3.35) and that one of the reference 3YSZ (Fig 3.25) shows that the densified 3YSZ still has a tetragonal structure after annealing. Fig 3.36 and 3.37 show the XRD pattern of the densified 3% YSZ at 1400 °C after being annealed with a higher precision at around 50 degrees and 60 degrees.
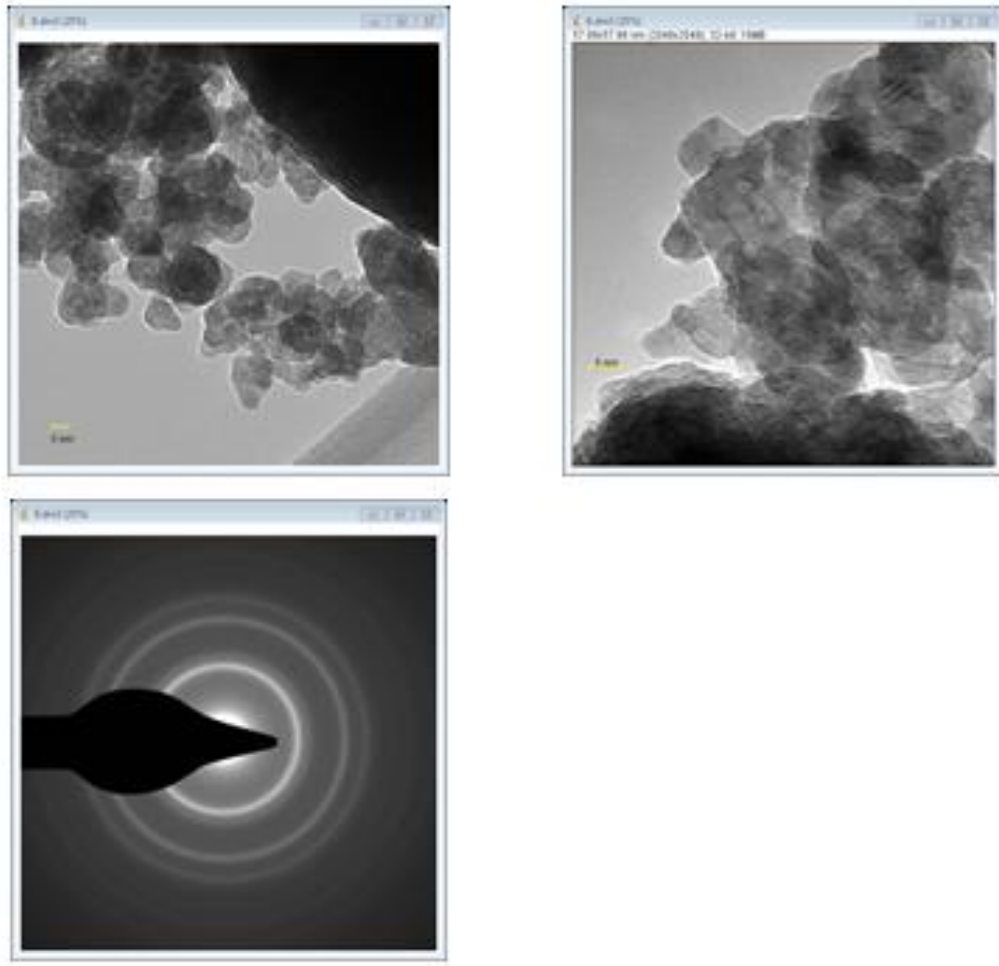
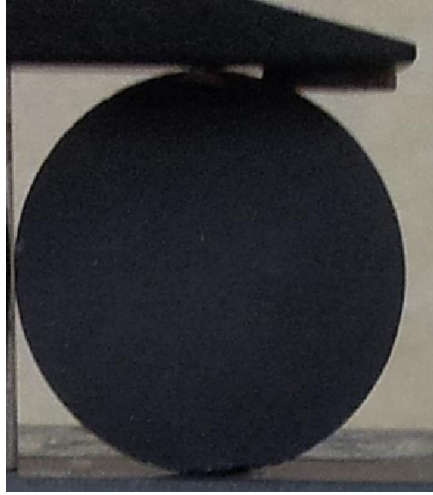Fig 3.33: TEM results for 3YSZ powder after baking at 550 °C for 3.5 hours

Figure 3.34: Densified 3YSZ without annealing

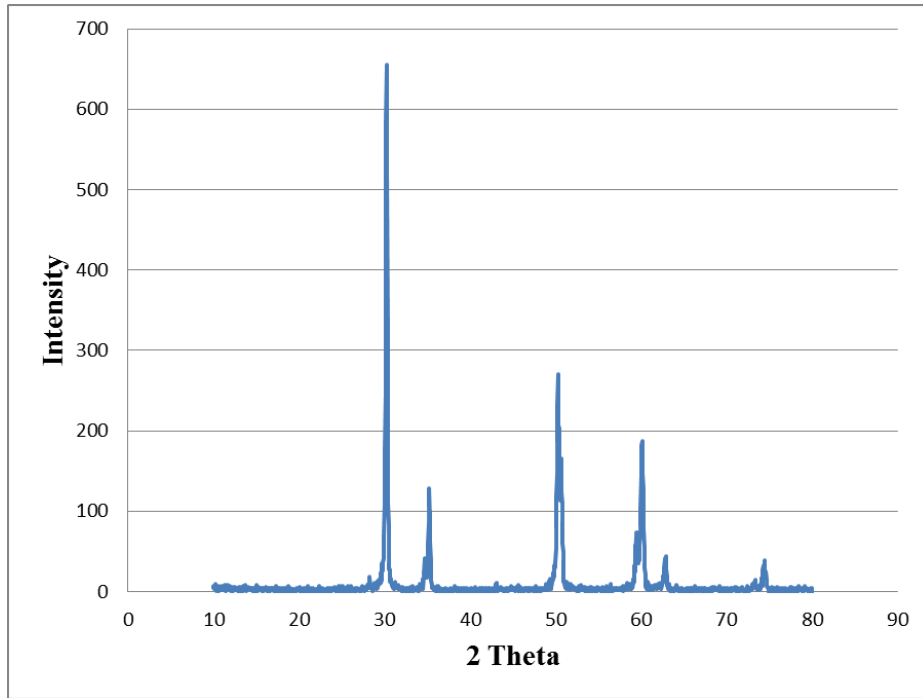Figure 3.35: light passing through the annealed 3YSZ sample

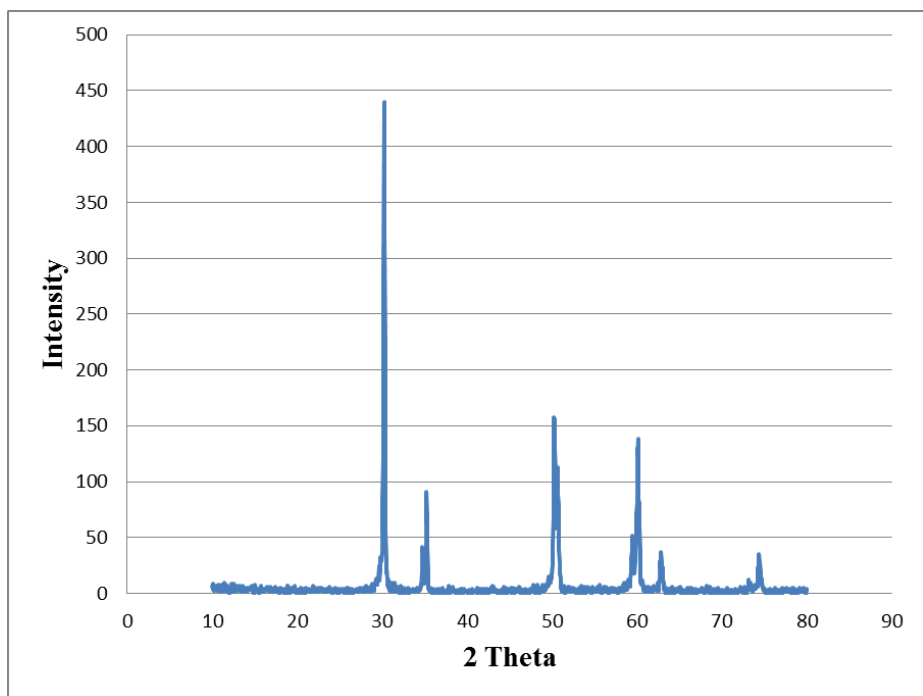Fig 3.36: XRD results for the densified 3% YSZ at 1400 °C after annealing

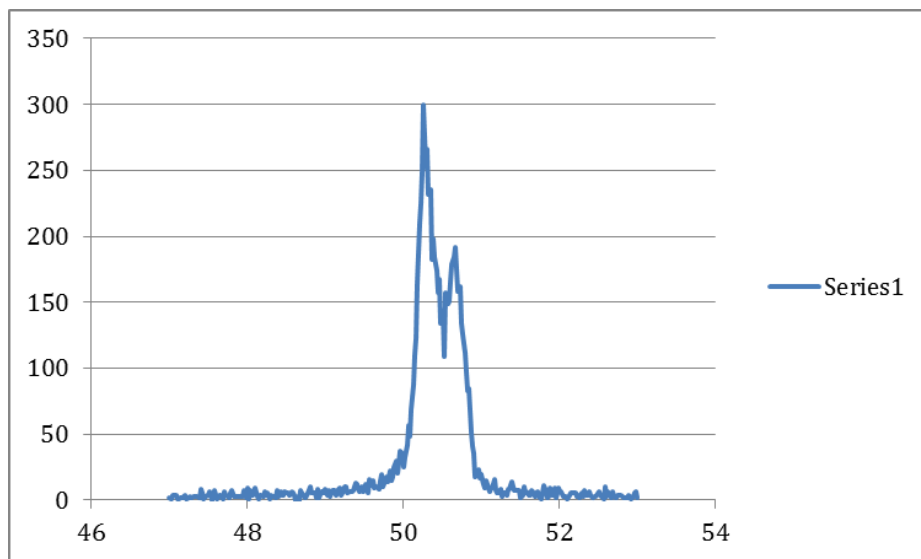Fig 3.37: XRD results for the densified 3% YSZ at 1400 °C without annealing

Fig 3.38: a subset of XRD pattern for the densified 3% YSZ at 1400 °C after annealing with higher resolution at around 50 degrees.
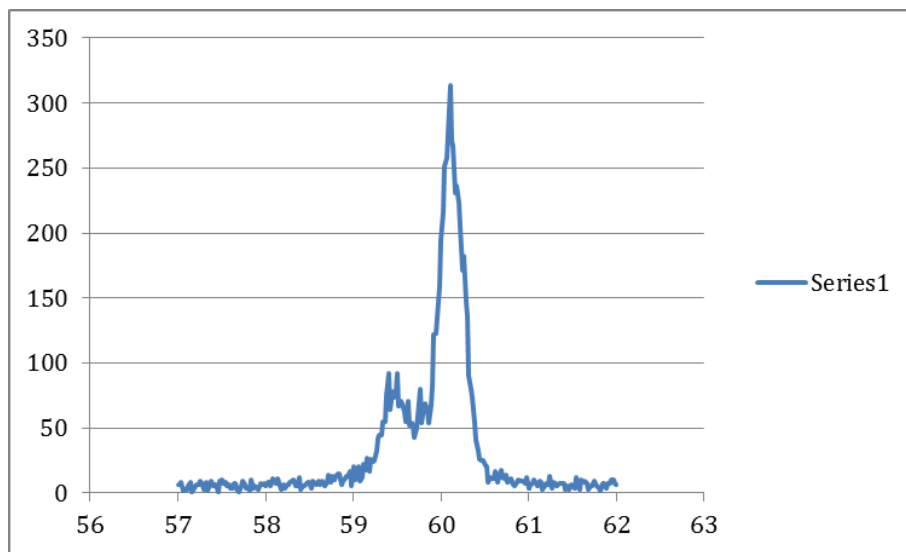

Fig 3.39: a subset of XRD pattern for the densified 3% YSZ at 1400 °C after annealing with higher resolution at around 60 degrees.

Refrences

[1] Nikander K., Sanders M., MEDICAMUNDI 54/3, (2010).

[2] Gussman, R.A., Am. Ind. Hyg. Assoc. J (45), (1984).

[3] May K.R. J. of Aerosol Science, Vol. 4, #3, p. 235, (1973).

[4] Gazzoli D., Mattei G., Valigi. M, J. Raman Spectrosc. 38: 824–831, (2007).

[5] Alaniz J.E., Perez-Gutierrez F.G., Aguilar G., Garay J.E., Optical Materials 32 (2009).

[6] Savioni B., Ballesteros C., Munoz Santiuste J.E., Gonzalez R., Chen Y., Physical Review B 57, 13439 (1998).

Chapter 4

Conclusions and recommendations for future work

A new approach to produce Yttrium stabilized Zirconia is introduced and the experimental results of characterizing these nanoparticles are presented. Different methods of producing YSZ are analyzed and among them the spray pyrolysis method as well as its advantages over other methods is explained in detail. The spray pyrolysis is the selected method in this thesis for its higher efficiency. The experiments started by investigating various potential precursors for preparation of zirconia and yttria stabilized zirconia (YSZ) nanoparticles, that yielded zirconium (IV) acetylacetonate $(C_5H_7O_2)_4Zr$ and yttrium (III) acetate hydrate $(CH_3CO_2)_3Y.xH_2O$ solved in methanol as the optimum precursors. Several atomizers including, ultrasonic nebulizer, fuel injector, collison nebulizer, and airbrush are examined to make the droplets. Among these atomizers, collison nebulizer and airbrush are used throughout the experiments for having higher rate of powder production. Using Nitrogen gas and a vacuum pump, droplets carried into a furnace and decomposed to form a powder there. The produced powder is accumulated on a special filter at the output of the furnace with the aid of the vacuum pump.

XRD method is primarily used to analyze the structure of the produced powders and the effect of furnace temperature on size distribution of the powders. It is observed that after a critical temperature, increasing furnace temperature results in the larger grain sizes, which is compensated by the increment in the efficiency of powder production. TEM images of the synthesized powder confirm the cubic structure of zirconia and tetragonal structure of YSZ. The final powders are densified using CAPAD technique through two sets of experiments. After getting a low 60% densification at the first experiment, the powder is baked before densification in the second experiment that results in a desired 99.999% densification. Raman Spectroscopy is administered on the final products, which verified the tetragonal phase of the densified YSZ. EDS/SEM spectrum also verifies the presence of YSZ at the intended concentrations.

For the future work, starting the experiment with a high purity precursor is recommended. This could potentially affect the structure and characteristics of the synthesized powders. Furthermore, the impurities might reduce the transparency of the densified sample by creating inhomogeneous absorption and scattering centers in the crystal. The impurity content of the samples can be determined using ICP (inductively coupled plasma).

The other improvement is to increase the efficiency of powder synthesis. There are different approaches to realize this, which should be analyzed along with their limitations in further detail. Changing the solvent, modifying the equipment or parts of the current SP setup are recommended as the initial steps.